CHAPTER 3.

RESULTS.

3.1 Introduction.

This chapter describes the results obtained from a series of batches of tablets made with unique combinations of formulation and manufacturing conditions. The derivation of the formulations, and the tabletting and testing methods are described in Chapter 2. The data identifying the individual batch parameters which were necessary for the inclusion of the results in a designed experiment are also given in this Chapter, although the analyses of these results are considered in subsequent chapters.

3.2 Particle size of Paracetamol.

The result of a particle size analysis of a powder depends on the material, the measuring technique and the model to which the experimental results are fitted. The most suitable parameter chosen to represent the size of a given material is that which most accurately reflects the characteristics of the powder under consideration. This study was essentially concerned with the surface effects of particles, either in relation to bonding to other particles or the interaction of the particles with liquids. The mean surface-volume diameter determined by Fisher sub-sieve sizing was considered to be the most suitable measure of the particle size of the materials used. This method does not however give any indication of the particle size distribution. The distributions derived from the Ferets diameter, the equivalent projected area diameter and the diameter determined by laser diffraction were therefore also determined. The mean result of three Fisher sub-sieve size analyses of the two size fractions of paracetamol are shown in Table 3.1.

Table 3.1.

The increase in surface-volume diameter (μm) of two size fractions of paracetamol with decreasing porosity on a Fisher sub-sieve sizer.

Porosity	0.75	0.70	0.65	0.60	0.55	0.50	0.45	0.40
+20 μm	14.0	20.4	21.0	20.4	22.4	26.0	29.2	31.6
-20 μm	3.7	7.4	6.7	7.3	8.3	8.2	8.8	10.5

It can be seen that the recorded size generally increased with decreasing porosity. An arbritary porosity of 0.6 was therefore chosen for comparison with the other excipients. The mean surface-volume diameter of the drug fractions and the excipients, each based on three determinations, are shown in Table 3.2.

Table 3.2.

Mean surface-volume diameters determined by Fisher sub-sieve sizer at a porosity of 0.6.

Material	Mean surface-volume diameter (μm)
Paracetamol -20	7.3
Paracetamol +20	20.4
Avicel PH101	8.2
Maize starch	14.0
Magnesium stearate	2.5

The results of the Ferets diameter, MOPS projected area and the laser scatter methods of particle sizing (Section 2.3) are shown in Table 3.3. Figure 3.1 shows the particle size distributions plotted on log-probability paper, the MOPS projected area figures in each case being converted to the diameter of a circle of the same area by Equation 3.1 for comparison.

$$D = \sqrt{\frac{4.A}{\pi}} \qquad (3.1)$$

Where D is the diameter and A is the projected area.

The smaller size cut of paracetamol from the zig-zag classifier (Section 2.2) gave a slightly better fit to a log-normal distribution than the larger size material, but estimates of the geometric standard deviations for both fractions have been included for comparative purposes.

Table 3.3.
The geometric mean diameter (μm) (and geometric standard deviation) of two size fractions of paracetamol determined by different methods.

	Theoretical cut size	
Method	<20μm	>20μm
Ferets diameter	11.0 (2.3)	40.5 (2.1)
Projected Area	8.1 (2.4)	47.0 (2.1)
Laser scatter	15.6 (2.2)	59.0 (3.0)

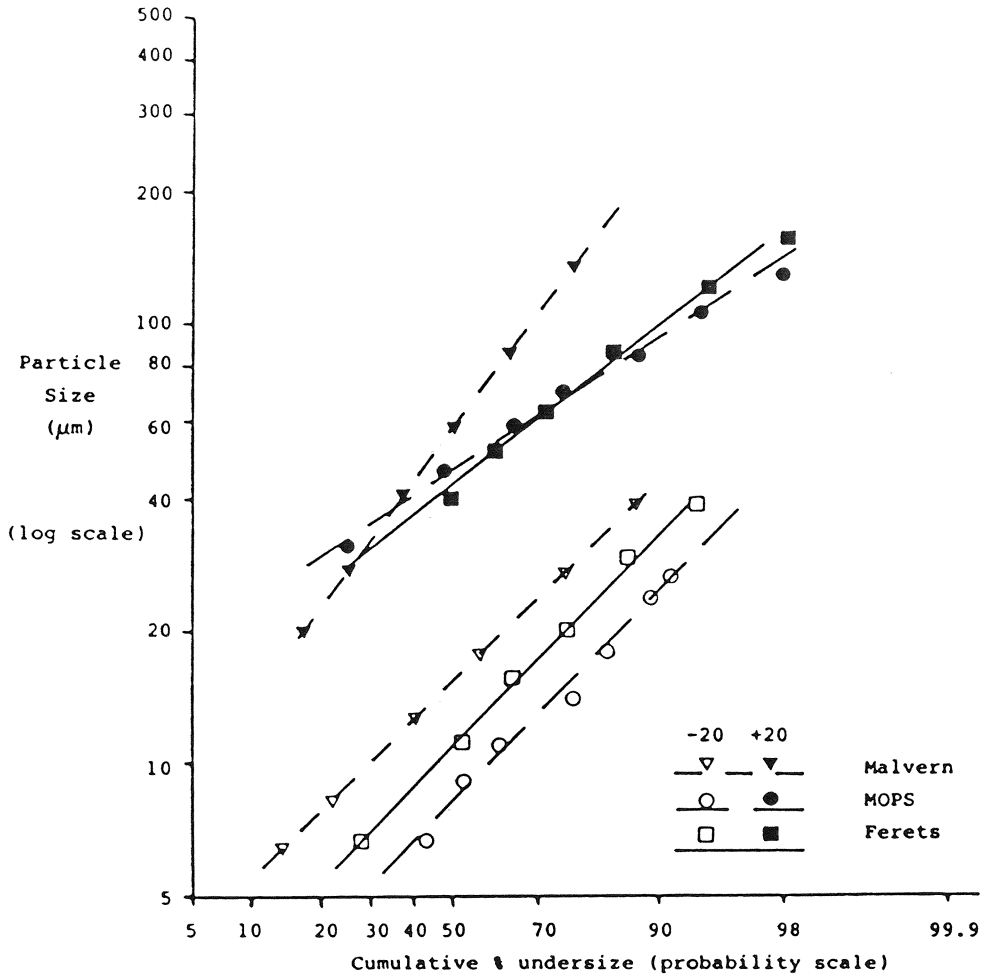

Figure 3.1

The particle size distribution of two size fractions of paracetamol determined by two microscopic methods (Ferets diameter and MOPS projected area/equivalent circle diameter) and a laser scatter method (Malvern).

The discrepancy in the particle size determined by the Fisher method compared to the other methods was due partly to the different characteristics of the crystals which were measured, and partly to the distribution model. For example, if a log-normal model with spherical particles is assumed, then the Hatch-Choate equations may be applied to convert a volume distribution to a number distribution (Allen 1975). An examination of Figures 2.2 and 2.3 shows that this type of conversion would not be applicable because of the acicular shape of the particles. The lower particle size of the +20μm fraction determined on the Fisher sub-sieve sizer compared to the other methods may arise due to the susceptibility of the powder to fracture during the measurements. This problem is recognised in the British Standard on air permeability methods, (B.S. 4359:Part 2 1971).

3.3 The Particle size of Aspirin.

The two fractions of aspirin were prepared by means of a sieve method, (Section 2.2). There was little to be gained by examining the size distribution of such samples and the fractions were outside the normal range of the Fisher sub-sieve sizer. A direct comparison of the particle size of aspirin and paracetamol was not therefore attempted.

3.4 Tablet manufacture and testing.

Tablets were manufactured according to the methods described in Section 2.5. The modified Hobart mixer and 12.5mm flat-faced punches were used in all cases. The results are presented with a drug and batch reference number which identify a formulation and a set of manufacturing conditions. These are defined in Table 3.4, with the associated formulations in Table 3.5.

The order of mixing and of manufacturing were determined by means of a computer random number generator to minimise any time sequence effects. Tablets for diametral compression, friability, dissolution and liquid uptake testing were also selected at random, after the exclusions described in Section 2.5, to provide a fair representation of the characteristics of a batch.

It was noted during the preparation of these formulations that for mixes containing the small particle size paracetamol, there was some adhesion of powder to the mixer wall. Consequently the mixes were assayed for paracetamol content, (BP 1980). The mean results of duplicate assays are shown in Table 3.6. In the case of aspirin no powder losses were noted.

Table 3.6 together with Table 3.4 confirms that paracetamol losses were restricted to mixes containing smaller particle size drug; there is also evidence that longer mixing times gave greater adhesion of drug to the mixer. The adherent material was almost certainly composed of the highly electrostatic 'fines' of the drug fraction.

TABLE 3.4

The Manufacturing Parameters Used in the Production of Batches of Paracetamol and Aspirin Tablets.

BATCH CODE	PARTICLE SIZE **	MIXING TIME mins	STARCH CONCENTRATION %	COMPACTION PRESSURE MNm^{-2}
1	large	1	1	100
2	large	1	1	150
3	large	1	1	200
4	large	5	1	100
5	large	5	1	150
6	large	5	1	200
7	large	1	7	100
8	large	1	7	150
9	large	1	7	200
10	large	5	7	100
11	large	5	7	150
12	large	5	7	200
13	small	1	1	100
14	small	1	1	150
15	small	1	1	200
16	small	5	1	100
17	small	5	1	150
18	small	5	1	200
19	small	1	7	100
20	small	1	7	150
21	small	1	7	200
22	small	5	7	100
23	small	5	7	150
24	small	5	7	200

** Small or large paracetamol particles were under or over 20μm (Section 2.2). Small or large aspirin particles were the sieve fractions 300-355μm or 355-425μm respectively.

Table 3.5

The experimental formulations used for the manufacture of aspirin and paracetamol tablets.

Batch size 500g.

i. Low starch concentration formulation.

	%
Aspirin or Paracetamol	25.0
Avicel PH101	72.9
Maize Starch	1.0
Magnesium Stearate	1.0
Aerosil 200	0.1
	100.0

ii. High starch concentration formulation.

	%
Aspirin or Paracetamol	25.0
Avicel PH101	66.9
Maize Starch	7.0
Magnesium Stearate	1.0
Aerosil 200	0.1
	100.0

This phenomenon was considered to be an integral facet of the formulation and experimental design and, in order to keep the paracetamol content of the tablets the same, the tablet target weight for each mix was adjusted as shown in Table 3.6.

Table 3.6.

Assay figures for paracetamol tablets (BP 1980) and target weight for mixes.

batches	1-3	4-6	7-9	10-12	13-15	16-18	19-21	22-24
assay %	25.1	24.7	24.8	25.1	23.7	21.5	23.6	22.2
target weight(mg)	399	405	404	398	423	465	424	451

The dissolution results were all obtained using the Kontron apparatus and are based on the mean of six tablets. The mean tensile fracture stress was calculated from the breaking load of 14-20 tablets after excluding any tablets apparently failing to break in tension. The friability test was carried out twice for each batch of tablets using 20 tablets per test, the results being expressed as the average of the two tests. The liquid uptake values represent the mean of two or three determinations. The other values in the summary Tables 3.7 and 3.8 were means of 70 - 100 tablets.

TABLE 3.7

A Summary of the Experimental Results Relating to Paracetamol Tablets.

BATCH CODE	UPPER PUNCH PRESS. MNm^{-2}	TENSILE FRACTURE STRESS MNm^{-2}	T50% min	T60% min	T90% min	COEFF. WEIGHT VARN. %	TABLET DENSITY Kgm^{-3}	FRIAB-ILITY %	POROS-ITY %	LIQUID UPTAKE sec
1	108.8	0.915	9.0	12.2	30.9	1.32	1252.7	0.860	14.2	44.5
2	145.9	1.078	7.8	10.7	34.5	1.21	1279.3	0.668	12.4	64.0
3	195.2	1.121	6.8	8.9	30.2	1.04	1282.0	0.565	12.2	76.1
4	104.9	0.389	8.3	10.3	25.6	1.34	1225.9	5.749	16.0	131.1
5	157.3	0.537	6.3	7.8	18.4	1.72	1255.3	1.447	14.1	174.6
6	195.5	0.568	5.0	6.0	13.1	0.98	1270.7	1.708	13.0	179.7
7	94.3	0.678	2.2	2.5	4.0	1.05	1241.2	1.302	15.0	30.8
8	153.4	0.826	2.2	2.5	4.1	1.29	1274.7	0.983	12.7	54.6
9	208.4	0.849	2.5	2.8	4.8	0.89	1280.1	0.795	12.3	87.8
10	102.5	0.279	3.7	4.5	10.5	1.27	1210.9	39.118	17.1	148.1
11	156.9	0.416	3.9	4.6	9.5	1.45	1255.0	14.636	14.0	215.7
12	197.8	0.430	4.1	4.8	10.2	1.19	1259.4	11.143	13.7	212.3
13	98.4	1.169	11.2	14.2	31.7	2.77	1235.5	1.037	15.4	42.3
14	153.2	1.377	13.5	18.2	45.9	8.79	1253.2	1.376	14.2	68.4
15	192.2	1.496	14.4	20.0	57.3	10.77	1266.1	0.912	13.3	34.6
16	111.2	0.676	11.2	15.7	44.0	5.90	1229.2	2.916	15.8	80.5
17	135.9	0.825	17.5	25.4	60.2	3.17	1263.1	2.058	13.5	87.0
18	177.4	0.983	14.5	19.8	54.4	4.45	1280.6	1.058	12.3	173.1
19	90.1	0.919	4.8	6.0	14.1	5.03	1209.2	1.660	17.2	26.9
20	139.5	1.113	3.9	5.0	14.0	9.79	1237.9	1.243	15.2	43.1
21	214.9	1.369	3.7	4.8	13.7	9.37	1270.9	2.920	12.9	42.8
22	88.6	0.378	2.2	2.5	4.8	4.41	1184.6	10.060	18.9	59.6
23	129.2	0.640	2.6	2.9	5.6	2.41	1240.8	1.921	15.0	73.5
24	189.6	0.701	3.6	4.1	8.5	3.35	1259.0	2.078	13.8	152.4

TABLE 3.8

A Summary of the Experimental Results Relating to Aspirin Tablets.

BATCH CODE	UPPER PUNCH PRESS. MNm^{-2}	TENSILE FRACTURE STRESS MNm^{-2}	T50% min	T60% min	T90% min	COEFF. WEIGHT VARN. %	TABLET DENSITY Kgm^{-3}	FRIAB--ILITY %	POROS--ITY	LIQUID UPTAKE sec
1	99.4	0.950	28.6	35.2	77.0	2.37	1261.2	0.997	13.6	100.3
2	155.9	1.128	37.0	47.4	123.0	0.97	1314.1	0.818	10.0	170.6
3	226.1	1.244	31.6	41.0	120.5	0.97	1319.6	0.591	9.6	255.6
4	104.4	0.688	20.8	26.5	56.6	1.25	1251.1	1.399	14.3	37.3
5	168.3	0.850	18.6	23.9	52.5	1.13	1287.5	1.372	11.8	72.7
6	181.8	0.965	20.1	26.7	63.7	3.26	1289.9	0.851	11.6	37.5
7	109.3	0.815	17.3	22.3	49.0	1.19	1275.5	1.472	12.6	83.3
8	162.9	0.905	16.2	21.3	51.2	1.09	1301.8	1.101	10.8	71.8
9	213.5	0.967	17.3	23.0	53.9	1.13	1310.1	0.994	10.3	81.1
10	93.7	0.470	16.1	21.8	54.3	1.77	1235.6	2.686	15.4	19.0
11	166.0	0.634	14.3	19.2	46.1	1.17	1288.1	1.521	11.8	27.6
12	193.2	0.715	14.5	20.4	57.1	1.67	1294.1	1.273	11.4	31.2
13	103.6	0.916	28.6	35.6	82.3	0.83	1274.1	1.309	12.7	55.7
14	159.2	1.247	42.0	55.2	145.7	1.20	1315.6	0.764	9.9	123.8
15	199.5	1.146	30.9	40.3	124.2	1.09	1316.4	0.816	9.8	162.0
16	105.8	0.577	20.0	25.4	52.9	1.00	1252.5	1.886	14.2	27.7
17	140.1	0.844	20.5	26.0	57.0	0.93	1279.8	0.975	12.3	48.0
18	195.6	0.735	20.0	25.5	54.8	1.08	1297.1	1.188	11.2	35.9
19	107.8	0.857	16.7	21.3	44.3	1.26	1272.6	1.276	12.8	64.4
20	156.4	0.903	15.2	19.6	43.1	1.51	1298.7	0.802	11.1	87.0
21	170.8	0.882	14.1	18.5	40.8	1.07	1306.3	0.958	10.5	63.0
22	97.5	0.441	15.0	20.4	55.4	1.09	1230.8	2.896	15.7	15.3
23	161.3	0.737	14.9	19.6	44.7	1.38	1304.2	1.421	10.7	55.2
24	217.3	0.668	12.7	16.8	43.0	1.48	1293.4	1.868	11.4	47.3

The compaction pressure was found to be difficult to control, particularly with those batches which had poor flow properties. However, an analysis of the type used for the other tablet parameters, showed that the only significant treatment was the compaction pressure. This technique is described more fully in Section 4.1, but may be taken here as indicating that the discrepancies between the measured and target upper punch pressures did not affect the analyses applied to the other tablet parameters. The linear regression analyses of the intra-batch relationship between tensile fracture stress and upper punch pressure are summarised in Tables 3.9 and 3.10. This illustrates that some batches reached a limiting tensile fracture stress i.e. the gradient (tensile fracture stress/compaction pressure) decreased as the compaction pressure was raised within a group where the only difference was the compaction pressure. This will be discussed further in the subsequent chapters.

A problem similar to that with the compaction pressure was experienced with the tablet weight but the variation in this case was used as an index of the ability of a powder to flow from the hopper to the die. The coefficient of tablet weight variation has therefore been treated as an experimental variable, with the individual batch results presented in Tables 3.7 and 3.8. One consequence of the variable tablet weight was that individual tablets contained different amounts of drug. The dissolution data was therefore expressed as a percentage of the maximal release for each tablet tested, to overcome this variation.

Table 3.9

The linear regression analysis of the relationship between tensile fracture stress and compaction pressure for paracetamol tablets.

Batch Code	Mean Compaction Pressure (MNm^{-2})	Mean Tensile Fracture Stress (MNm^{-2})	Gradient (TFS/PRES)	Correlation Coefficient	Number of Tablets
1	108.82	0.915	0.0079	0.798 **	20
2	145.85	1.078	0.0040	0.580 *	16
3	195.22	1.121	0.0033	0.380	15
4	104.85	0.389	0.0032	0.763 **	19
5	157.33	0.537	0.0024	0.722 **	19
6	195.51	0.568	-0.0003	-0.041	17
7	94.30	0.678	0.0045	0.603 **	18
8	153.41	0.826	0.0001	0.020	18
9	208.35	0.849	-0.0014	-0.226	13
10	102.52	0.279	0.0039	0.833 **	19
11	156.93	0.416	0.0008	0.473 *	20
12	197.81	0.430	0.0002	0.072	14
13	98.44	1.169	0.0144	0.988 **	20
14	153.21	1.377	0.0076	0.926 **	20
15	192.16	1.496	0.0019	0.762 **	15
16	111.21	0.676	0.0068	0.980 **	20
17	135.95	0.825	0.0050	0.951 **	18
18	177.42	0.983	0.0028	0.892 **	18
19	90.89	0.919	0.0142	0.993 **	17
20	139.51	1.113	0.0068	0.942 **	18
21	214.94	1.369	0.0018	0.768 **	17
22	88.56	0.378	0.0067	0.978 **	19
23	129.21	0.640	0.0031	0.814 **	18
24	189.50	0.701	0.0025	0.854 **	14

significance levels; * $p < 0.05$, ** $p < 0.01$
TFS - Tensile Fracture Stress; PRES - Compaction Pressure

Table 3.10

The linear regression analysis of the relationship between tensile fracture stress and compaction pressure for aspirin tablets.

Batch Code	Mean Compaction Pressure (MNm^{-2})	Mean Tensile Fracture Stress (MNm^{-2})	Gradient (TFS/PRES)	Correlation Coefficient	Number of Tablets
1	99.4	0.950	0.0081	0.726 **	14
2	155.9	1.128	-0.0029	-0.671 **	14
3	226.1	1.244	0.0018	0.164	14
4	104.4	0.688	0.0041	0.532 *	14
5	168.3	0.850	-0.0007	-0.145	15
6	181.8	0.965	0.0005	0.116	15
7	109.3	0.815	0.0047	0.595 *	15
8	162.9	0.905	0.0055	0.589 *	15
9	213.5	0.967	-0.0012	-0.238	14
10	93.7	0.470	0.0081	0.697 **	14
11	166.0	0.634	0.0001	0.028	15
12	193.2	0.715	-0.0093	-0.248	14
13	103.6	0.916	0.0039	0.206	13
14	159.2	1.247	-0.0022	-0.216	15
15	199.5	1.146	-0.0020	-0.290	13
16	105.8	0.577	0.0067	0.749 **	13
17	140.1	0.844	0.0019	0.188	14
18	195.6	0.735	-0.0019	-0.298	15
19	107.8	0.857	0.0032	0.350	15
20	156.4	0.903	-0.0018	-0.371	15
21	170.8	0.882	-0.0010	-0.203	14
22	97.5	0.441	0.0050	0.488	14
23	161.3	0.737	0.0046	0.636 *	13
24	217.3	0.668	-0.0004	-0.097	11

significance levels; * $p < 0.05$, ** $p < 0.01$
TFS - Tensile Fracture Stress; PRES - Compaction Pressure

Tablet dissolution was examined according to a variety of models, the most promising of which were a first order and a cube root model. However, some of the batches were not adequately described by these models which led to the adoption of the views of Goldsmith et al. (1978) on the expression of dissolution data. These authors concluded that there is no great advantage in modifying the percentage of drug released versus time data. Analyses of the unmodified and first order dissolution rate data derived from the paracetamol tablets may be found in Sanderson et al. (1984), but dissolution model fitting will not be explored any further here.

Figures 3.2 to 3.17 show the dissolution profiles produced, the bars indicating 1 standard error of the mean. For clarity, only every tenth point is shown with the error bars slightly offset, but the lines joining the mean values are based on all the time points and were generated by the computer program described in Section 2.6.3. Tables 3.7 and 3.8 show the mean times for 50%, 60% and 90% drug release. It should be noted that the time scales in these Figures are not the same, with T90% times between 4 and 145 minutes (Tables 3.7 and 3.8), the more rapidly dissolving formulations could not be clearly shown with a single time scale.

Liquid uptake as determined by gamma-scintigraphy was used to give some indication of the initial phase of the dissolution process. The profiles shown in Figures 3.18 to 3.33 represent the percentage of the maximum count recorded within the initial tablet area at the mean time of the counting interval. Plate 3.1 illustrates the visual record obtained by this method. The profiles were based on the percentage of the

Plate 3.1

An example of the visual record obtained during the liquid uptake studies. The top left frame shows a 12.5mm tablet (black area) during the first 10s of contact with the radiolabelled liquid (coloured area). The subsequent frames show the following periods of 10s representing the first 40s of liquid uptake in total.

maximum count recorded in a circle defining the perimeter of the tablet in the first 10 seconds of liquid contact with the tablet, the time being taken at the middle of each counting interval (10s or 30s), and the count recorded as the mean count rate over that interval. It should be noted that the liquid uptake profiles, as with the dissolution, have different time scales for different groups of batches.

The mean, standard deviation and coefficient of variation for upper and lower punch pressures, weight, thickness, breaking load, tensile fracture stress, porosity, tablet density and relative density associated with each batch are shown the Appendix, Tables A.1 to A.48.

The remainder of this Chapter consists of the figures illustrating the dissolution and liquid uptake profiles obtained from individual batches. The combination of these results as part of a designed experiment is considered in the subsequent Chapters.

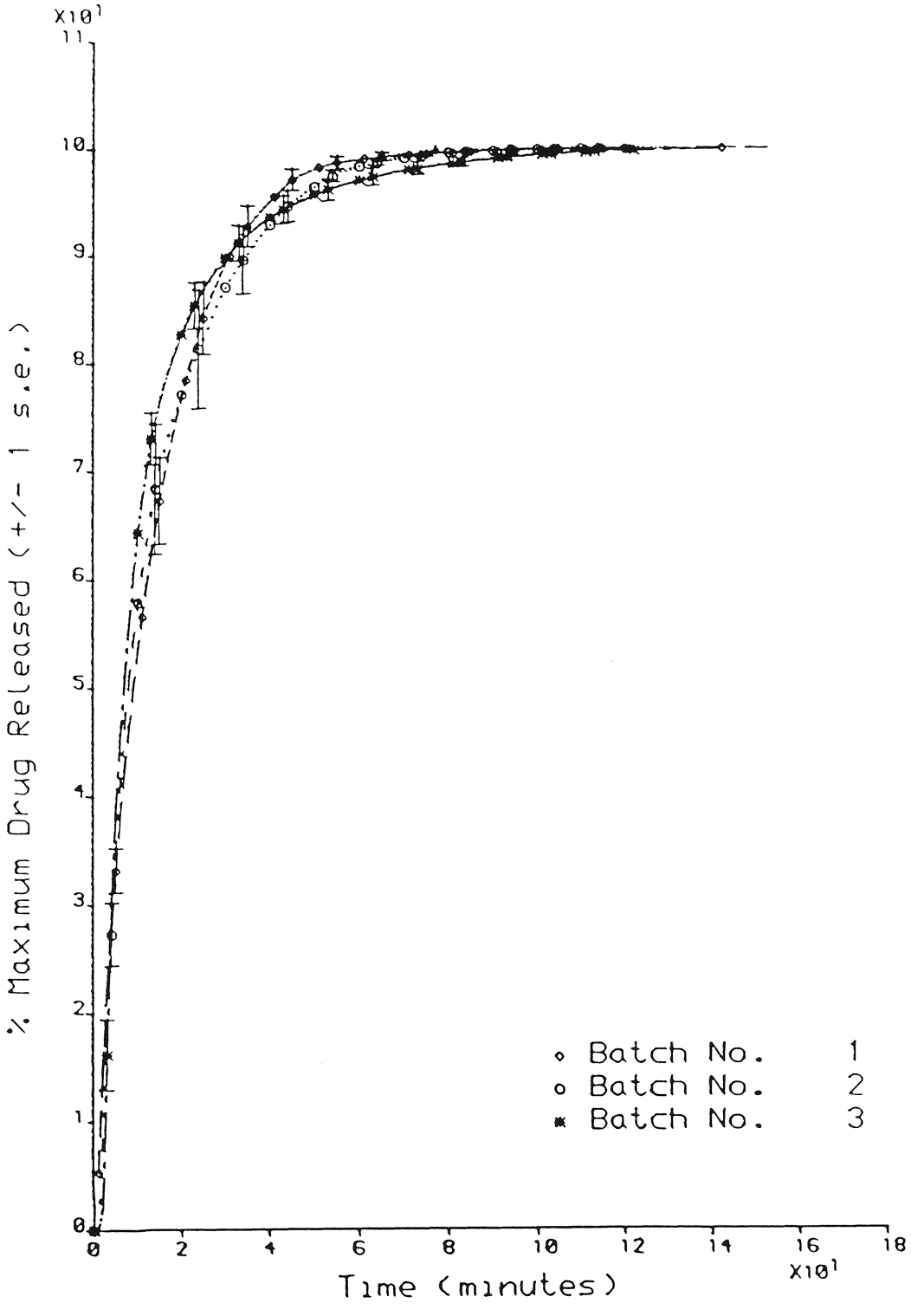

FIGURE 3.2

THE MEAN DISSOLUTION PROFILES FROM THREE BATCHES OF PARACETAMOL TABLETS (N=6).

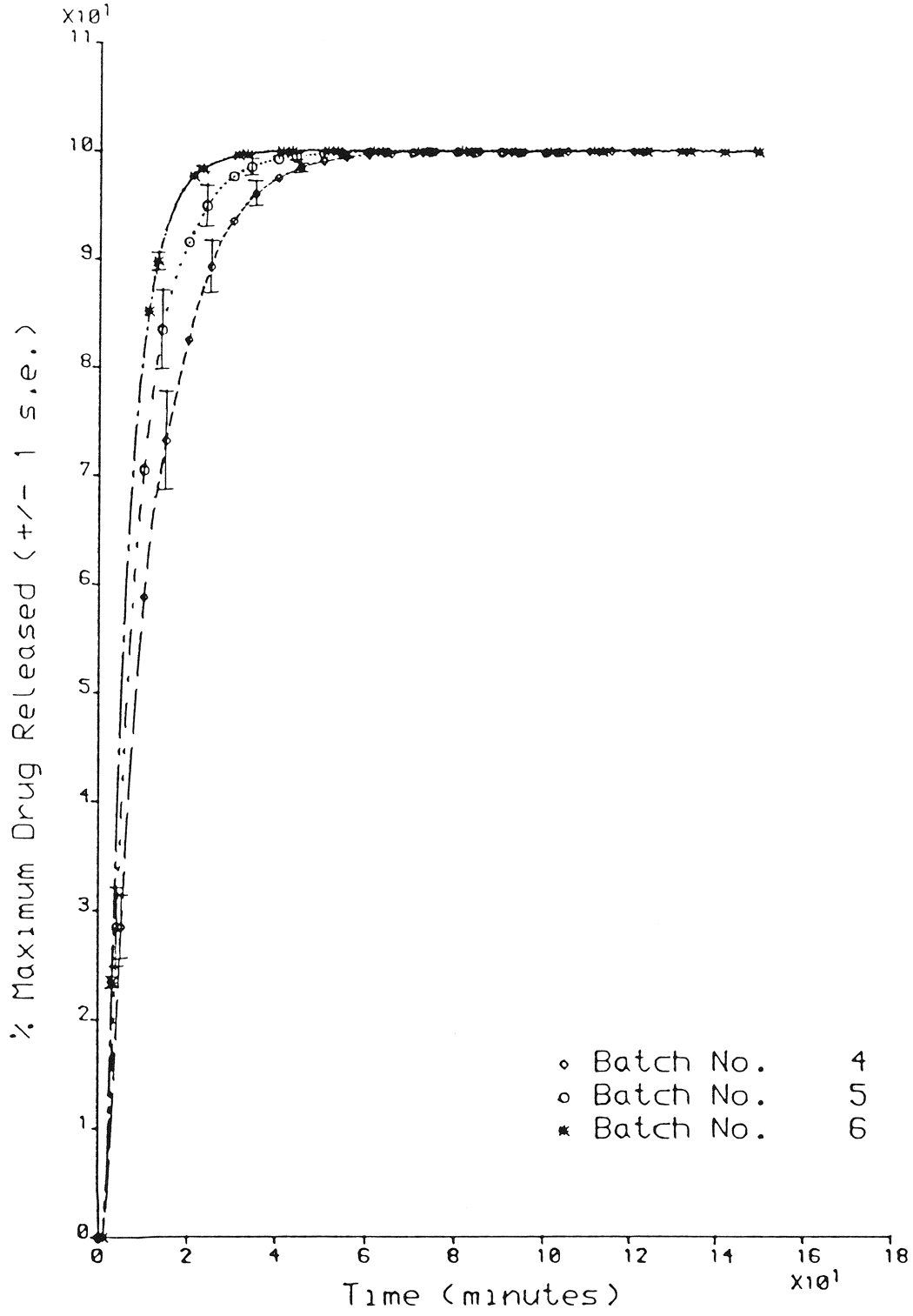

FIGURE 3.3

THE MEAN DISSOLUTION PROFILES FROM THREE BATCHES OF PARACETAMOL TABLETS (N=6).

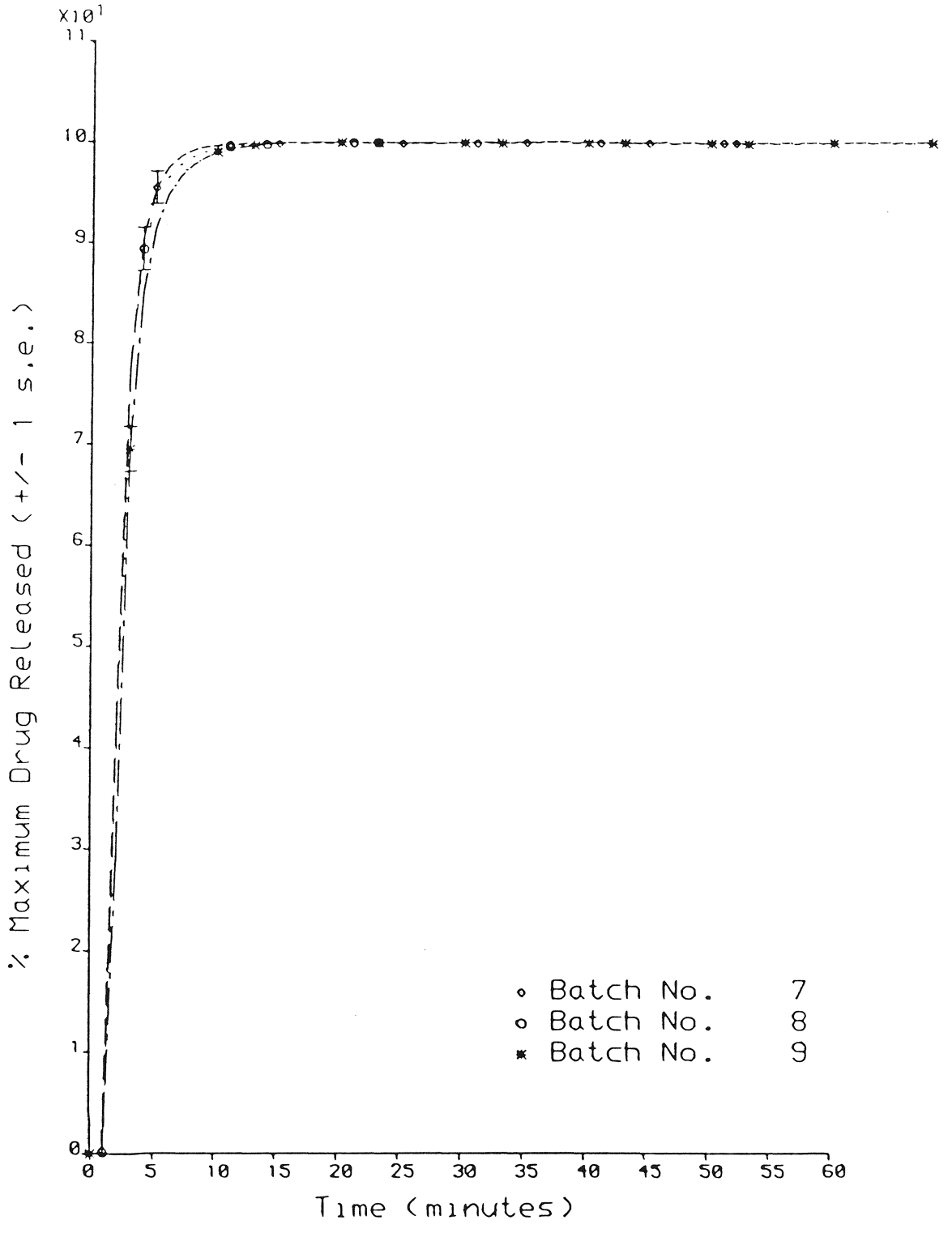

FIGURE 3.4

THE MEAN DISSOLUTION PROFILES FROM THREE BATCHES OF PARACETAMOL TABLETS (N=6).

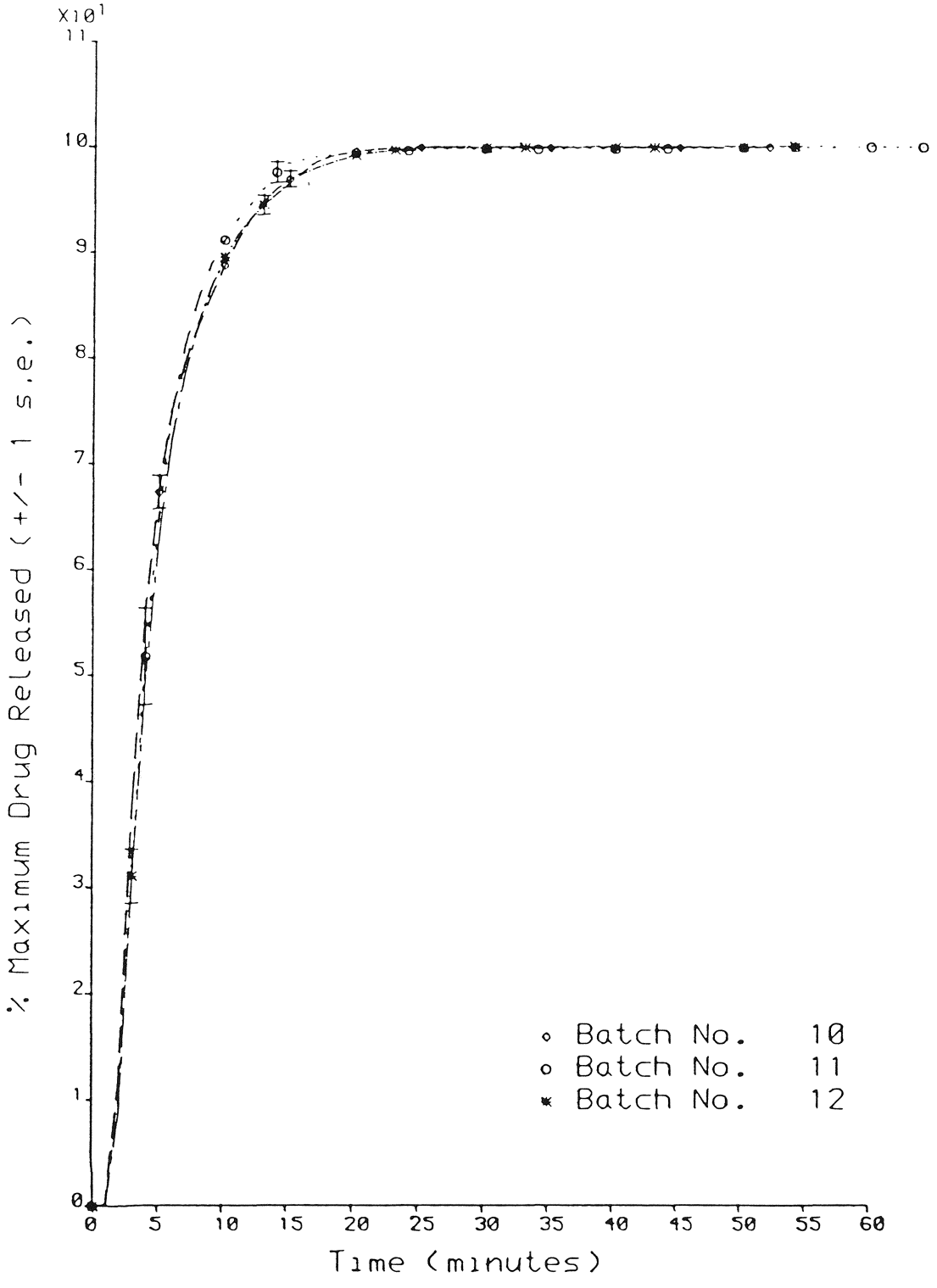

FIGURE 3.5

THE MEAN DISSOLUTION PROFILES FROM THREE BATCHES OF PARACETAMOL TABLETS (N=6).

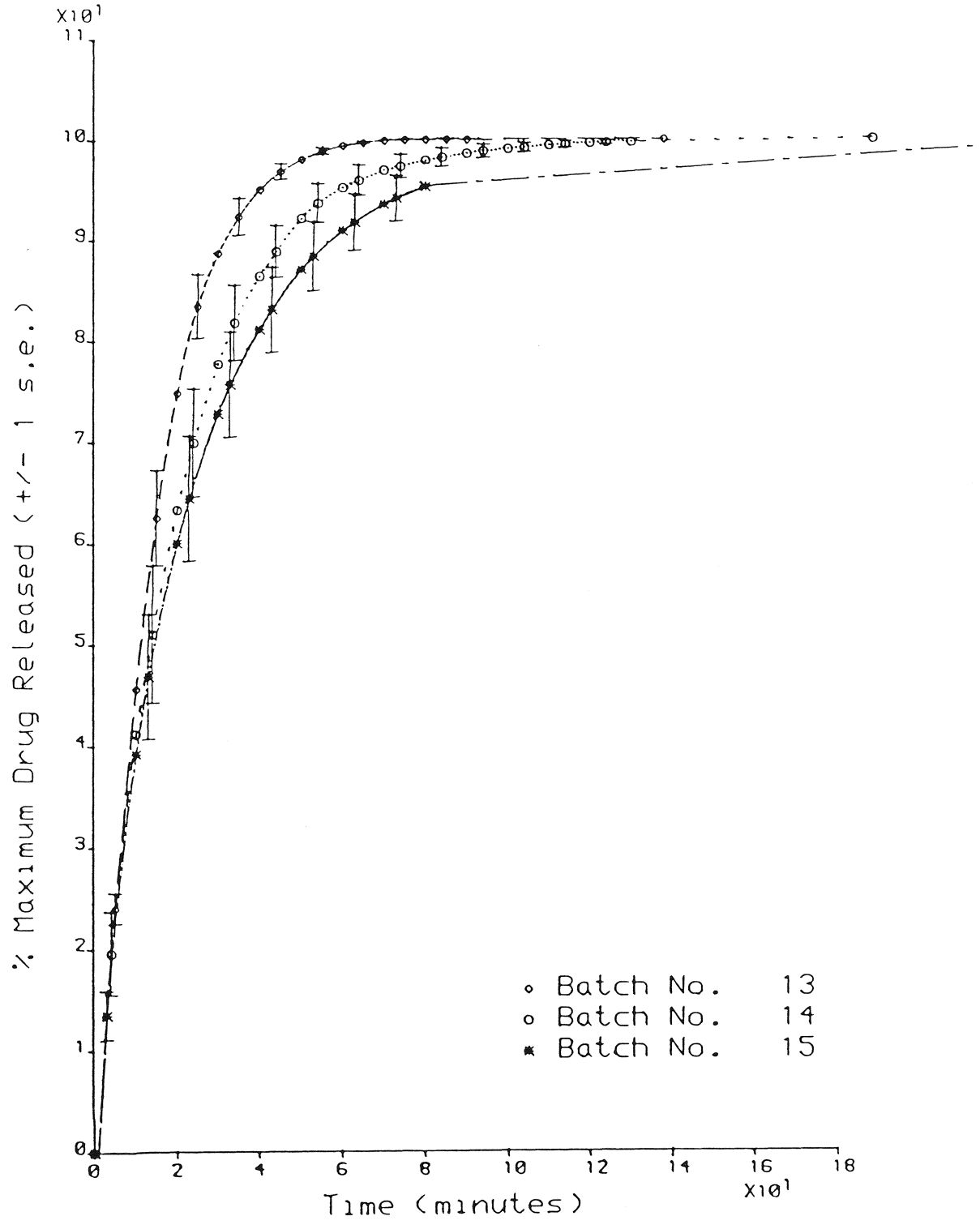

FIGURE 3.6

THE MEAN DISSOLUTION PROFILES FROM THREE BATCHES OF PARACETAMOL TABLETS (N=6).

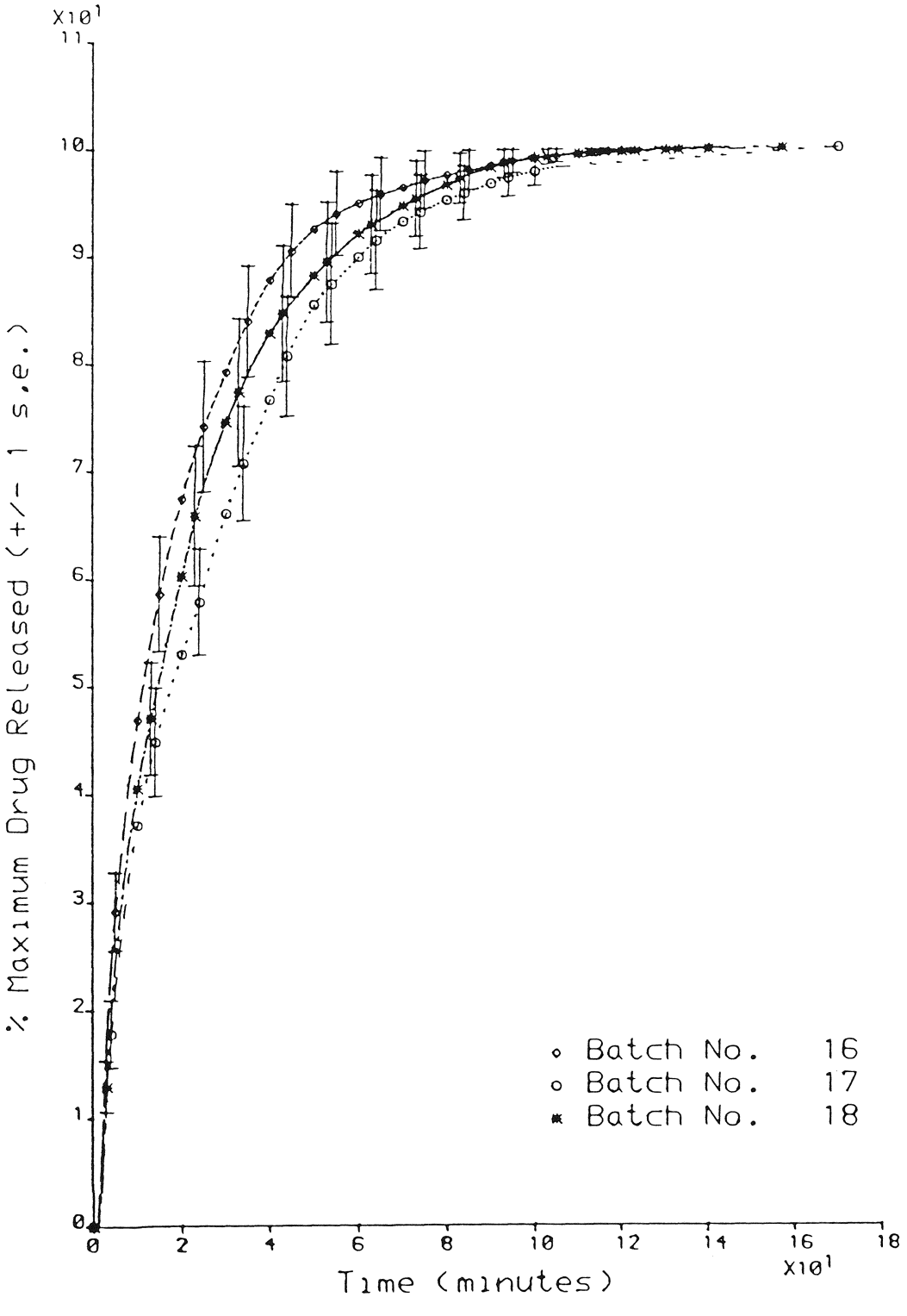

FIGURE 3.7

THE MEAN DISSOLUTION PROFILES FROM THREE BATCHES OF PARACETAMOL TABLETS (N=6).

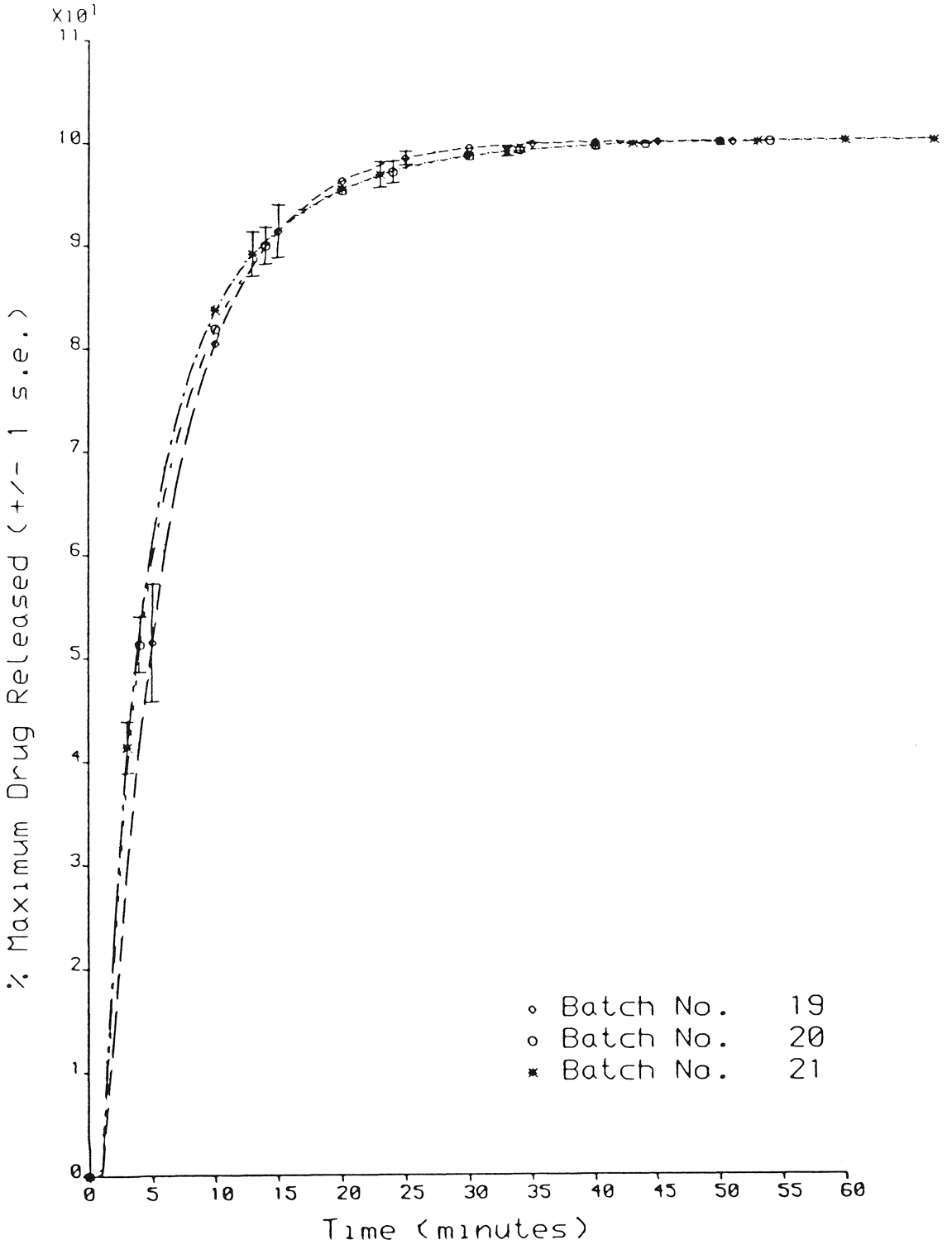

FIGURE 3.8

THE MEAN DISSOLUTION PROFILES FROM THREE BATCHES OF PARACETAMOL TABLETS (N=6).

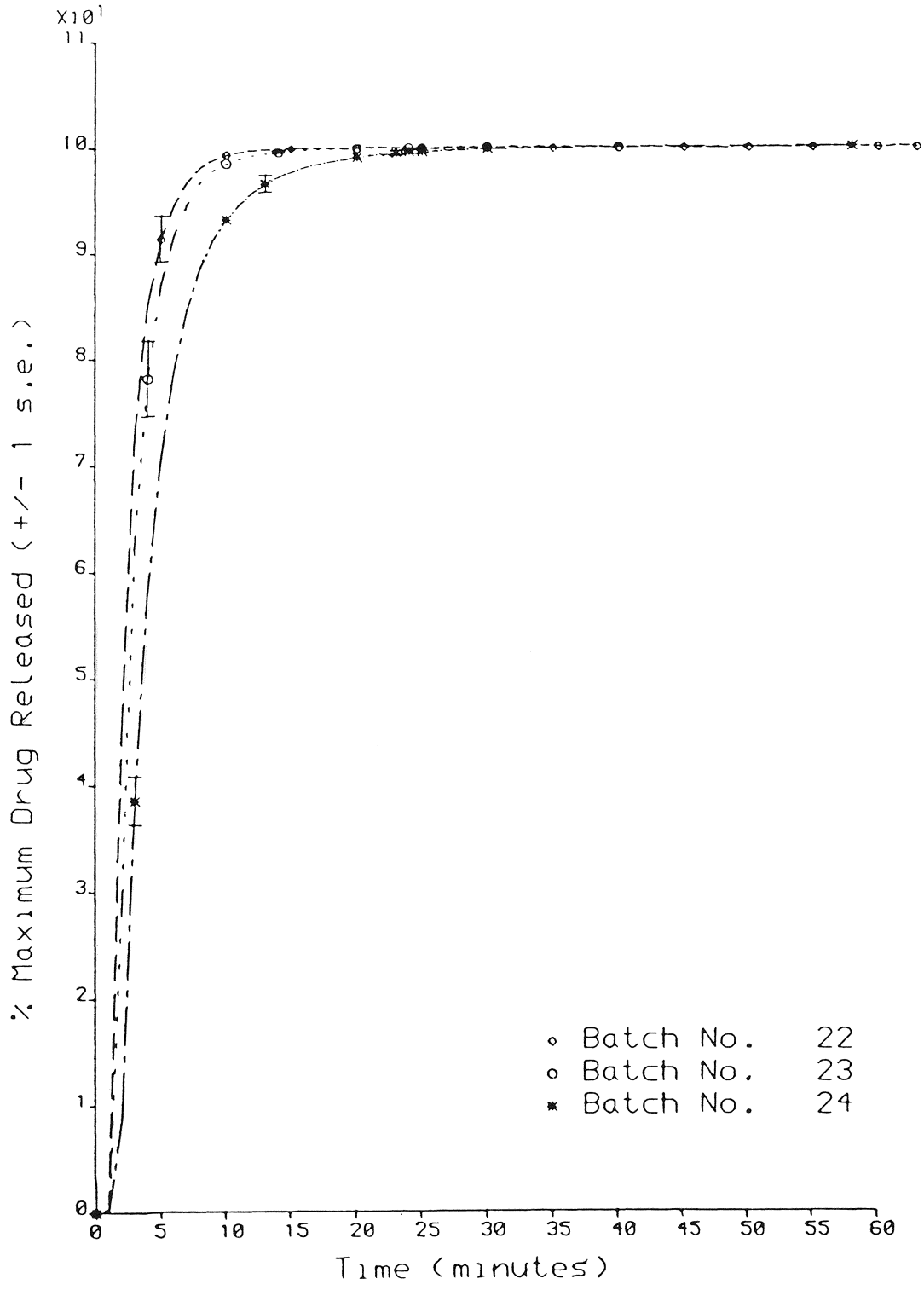

FIGURE 3.9

THE MEAN DISSOLUTION PROFILES FROM THREE BATCHES OF PARACETAMOL TABLETS (N=6).

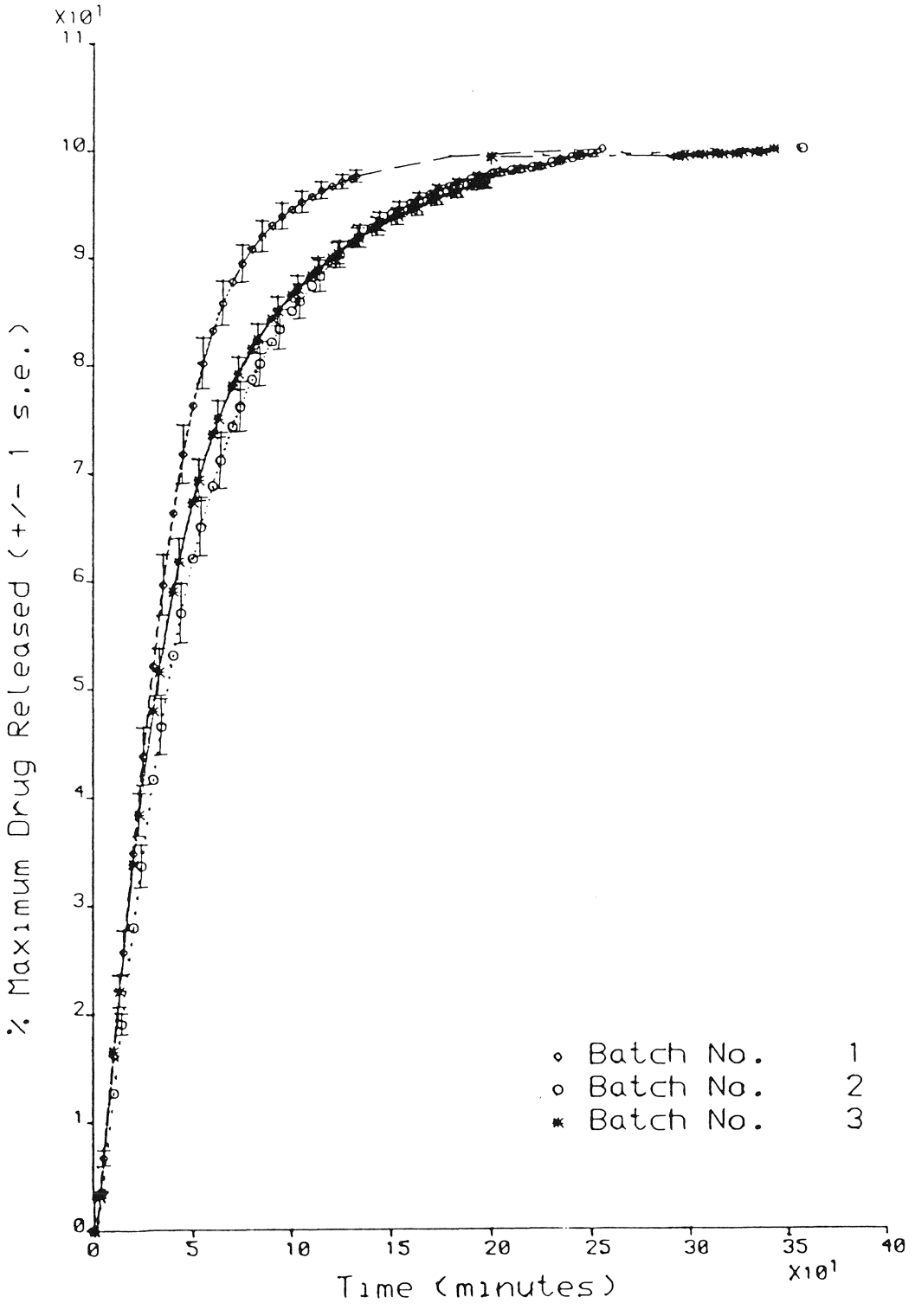

FIGURE 3.10

THE MEAN DISSOLUTION PROFILES FROM THREE BATCHES OF ASPIRIN TABLETS (N=6).

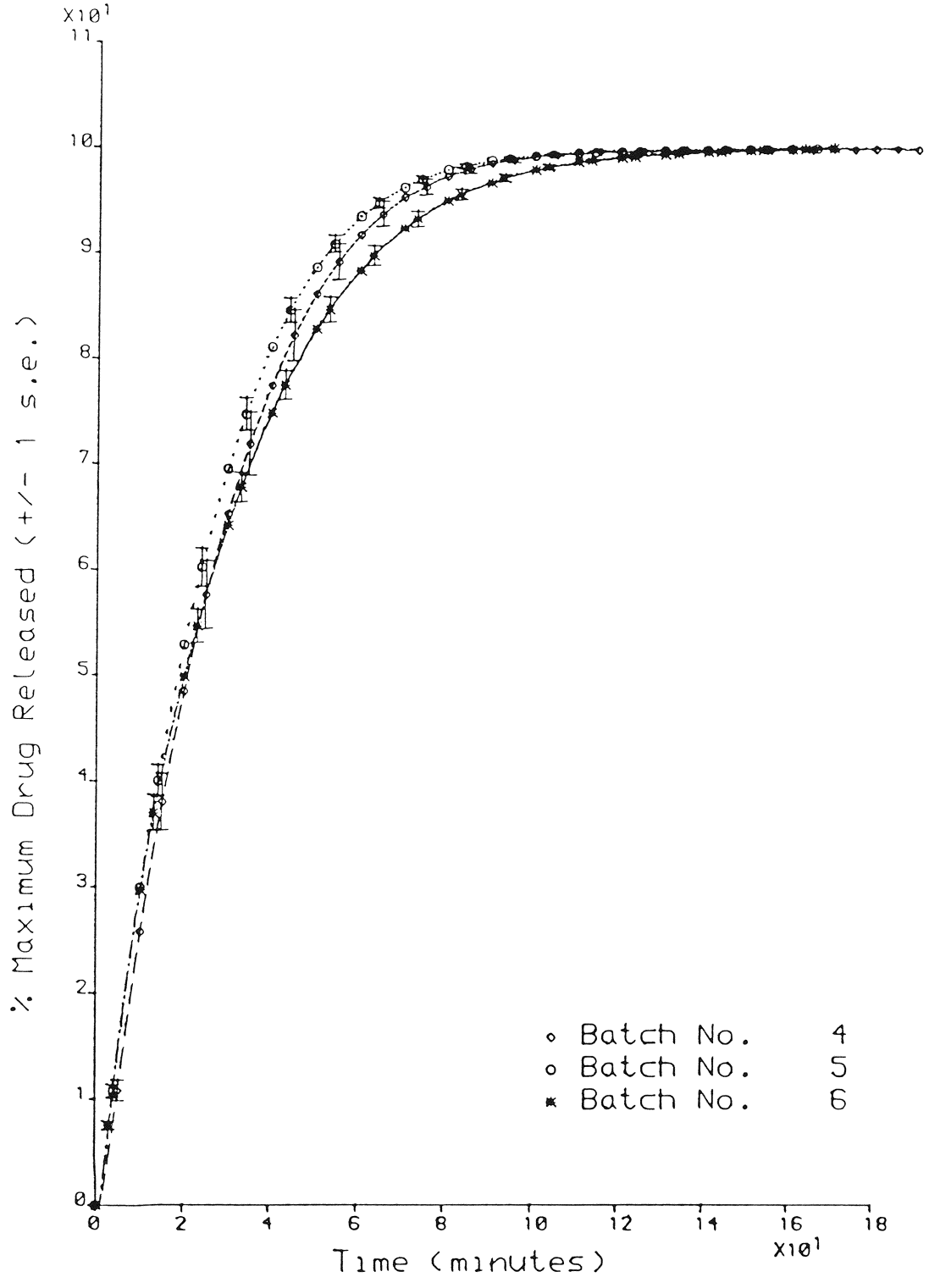

FIGURE 3.11

THE MEAN DISSOLUTION PROFILES FROM THREE BATCHES OF ASPIRIN TABLETS (N=6).

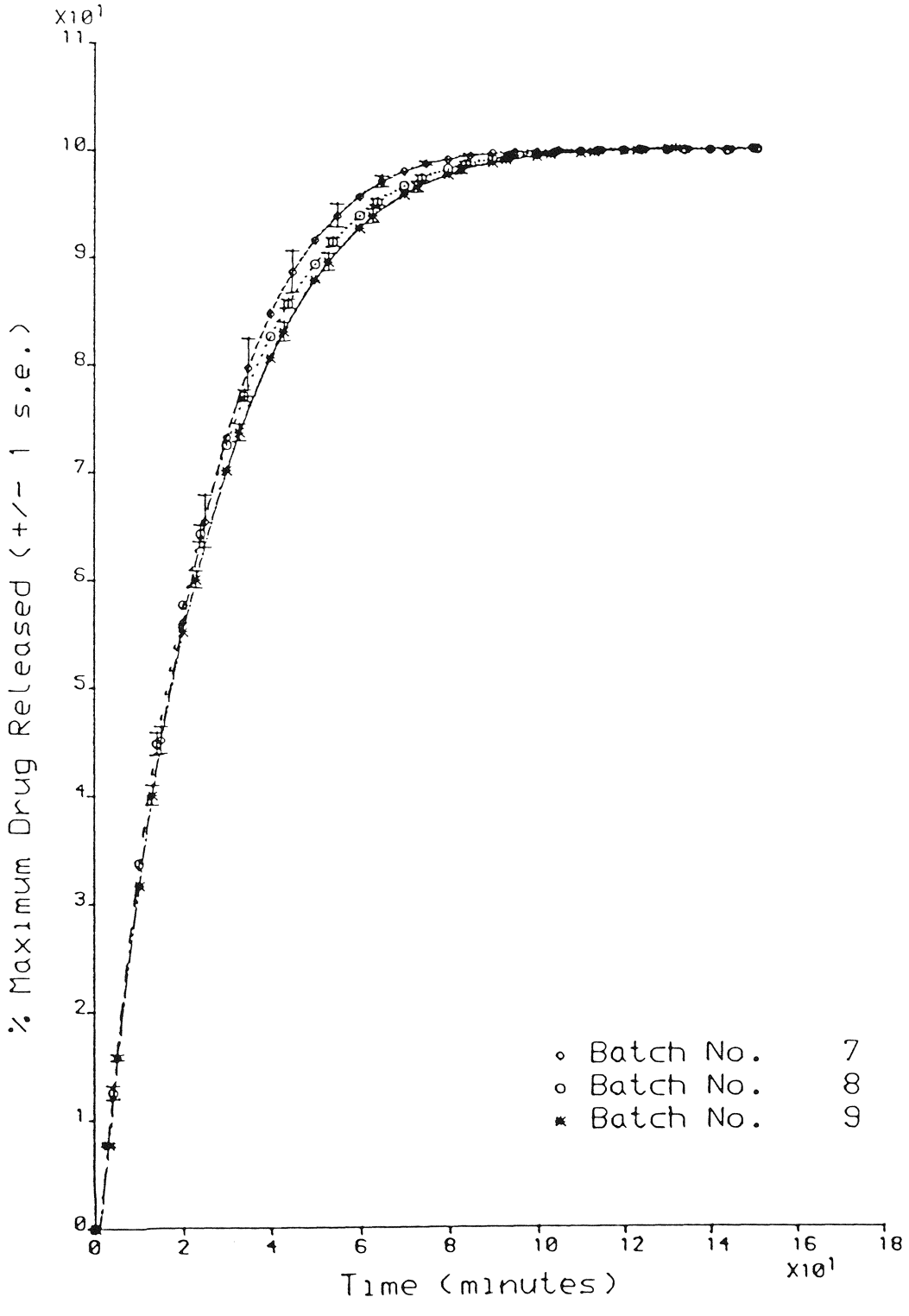

FIGURE 3.12

THE MEAN DISSOLUTION PROFILES FROM THREE BATCHES OF ASPIRIN TABLETS (N=6).

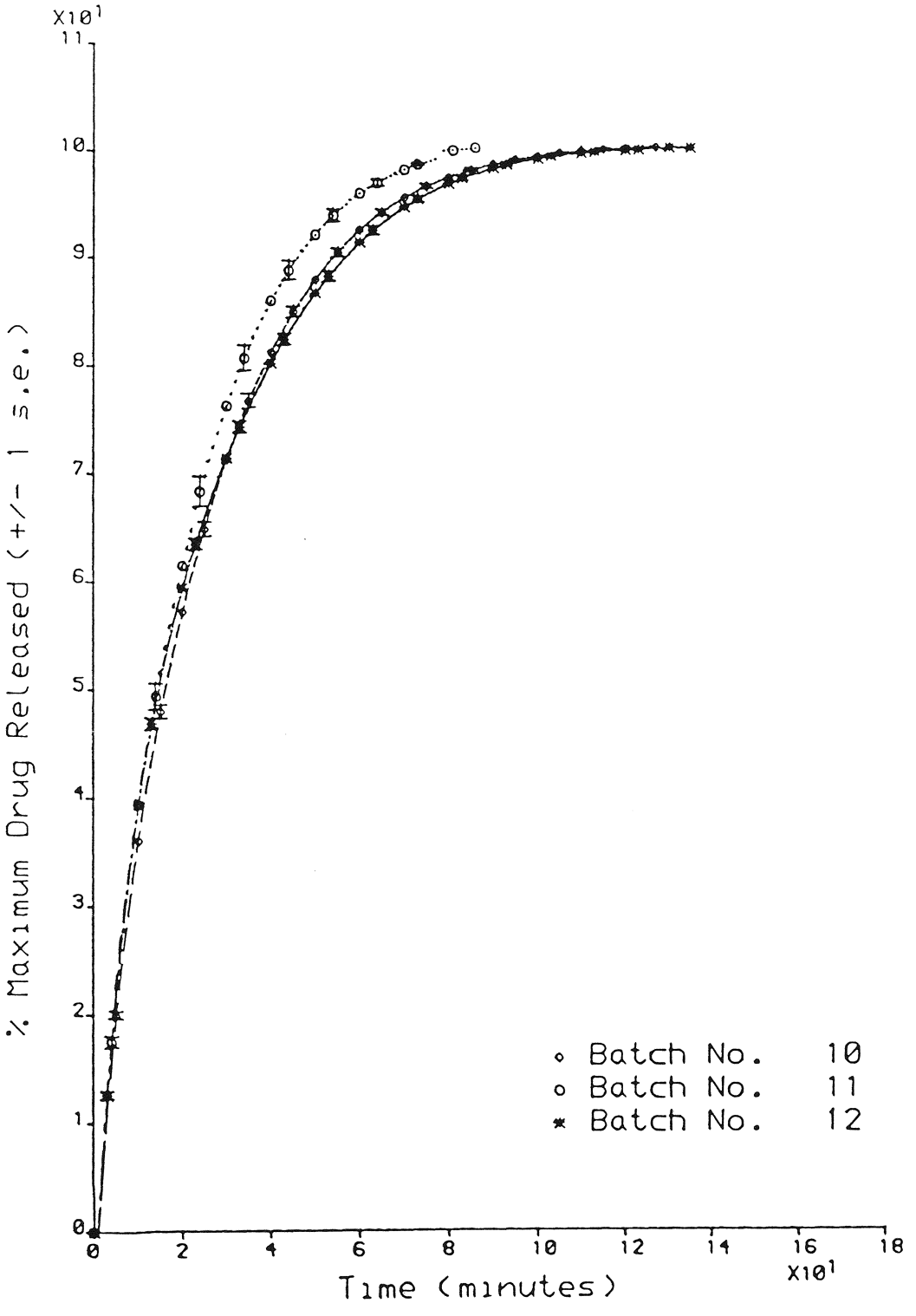

FIGURE 3.13

THE MEAN DISSOLUTION PROFILES FROM THREE BATCHES OF ASPIRIN TABLETS (N=6).

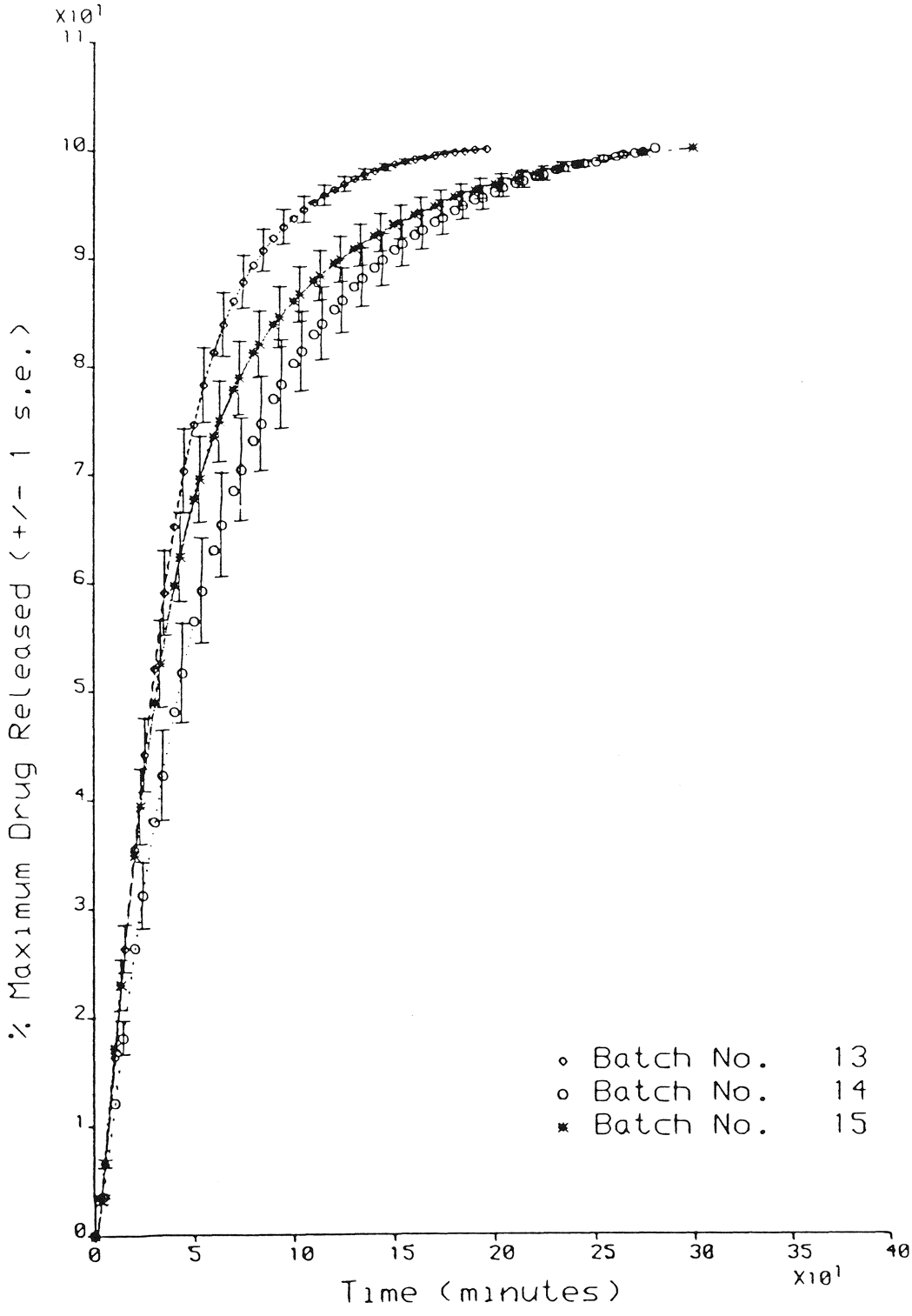

FIGURE 3.14

THE MEAN DISSOLUTION PROFILES FROM THREE BATCHES OF ASPIRIN TABLETS (N=6).

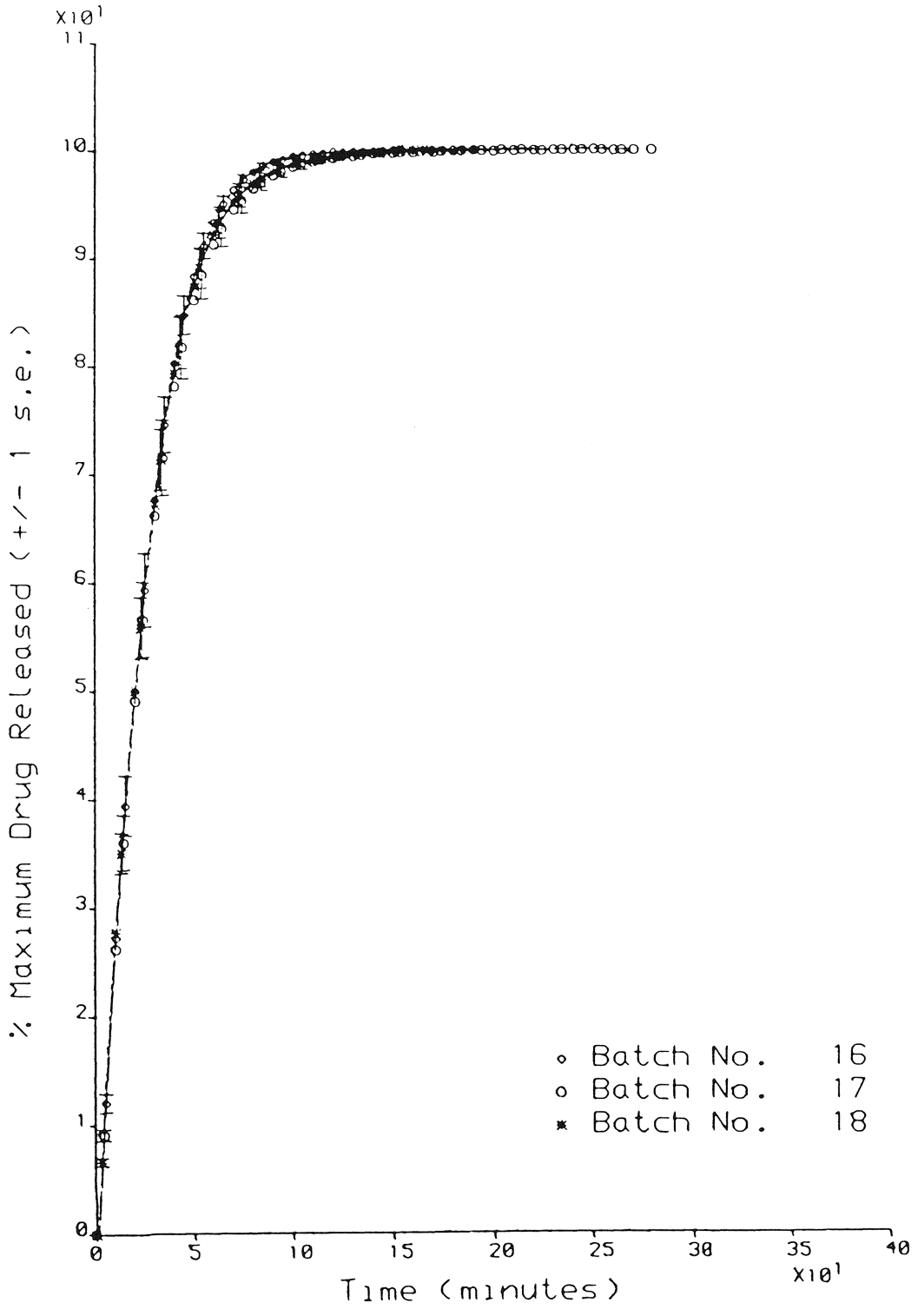

FIGURE 3.15

THE MEAN DISSOLUTION PROFILES FROM THREE BATCHES OF ASPIRIN TABLETS (N=6).

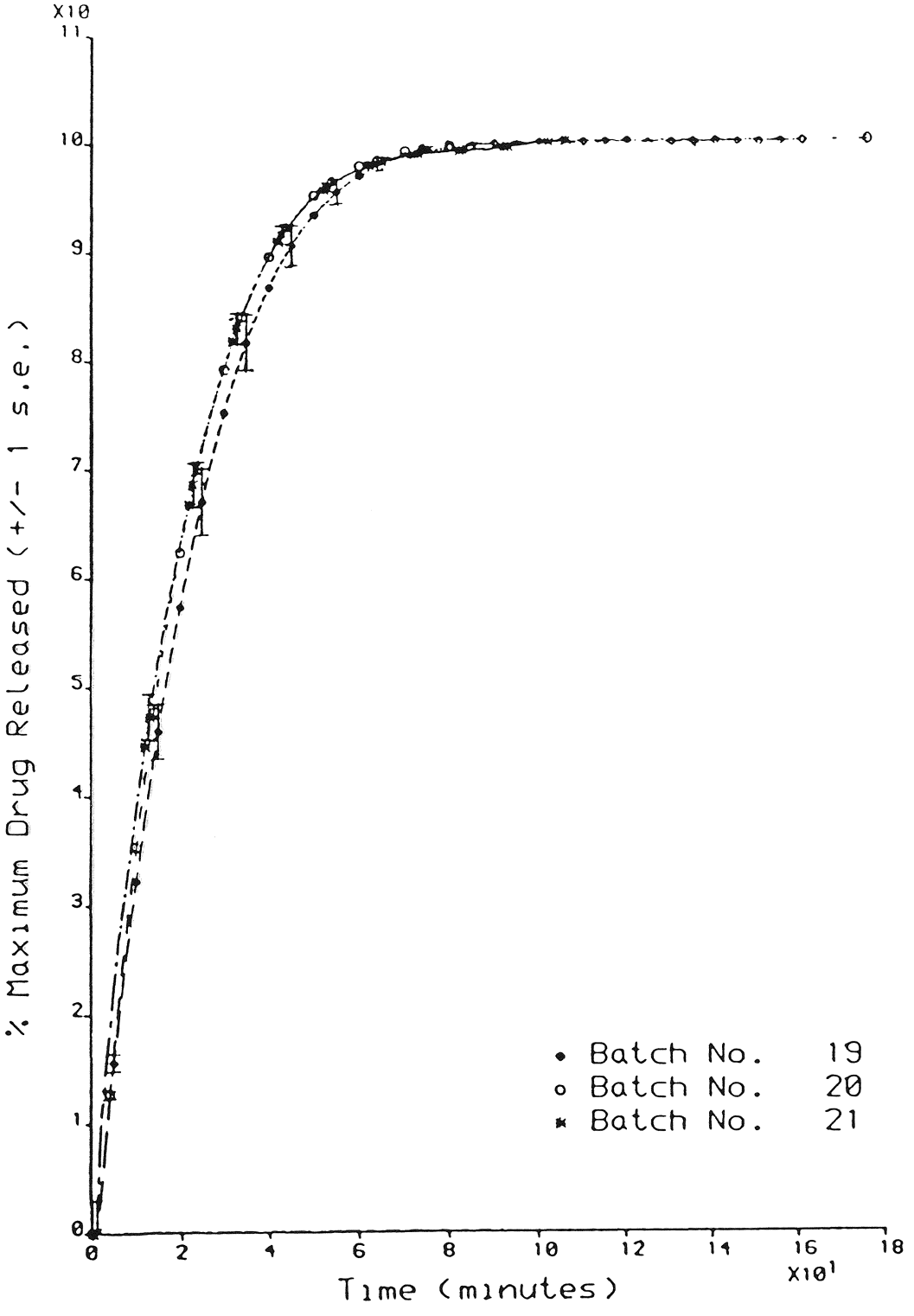

FIGURE 3.16

THE MEAN DISSOLUTION PROFILES FROM THREE BATCHES OF ASPIRIN TABLETS (N=6).

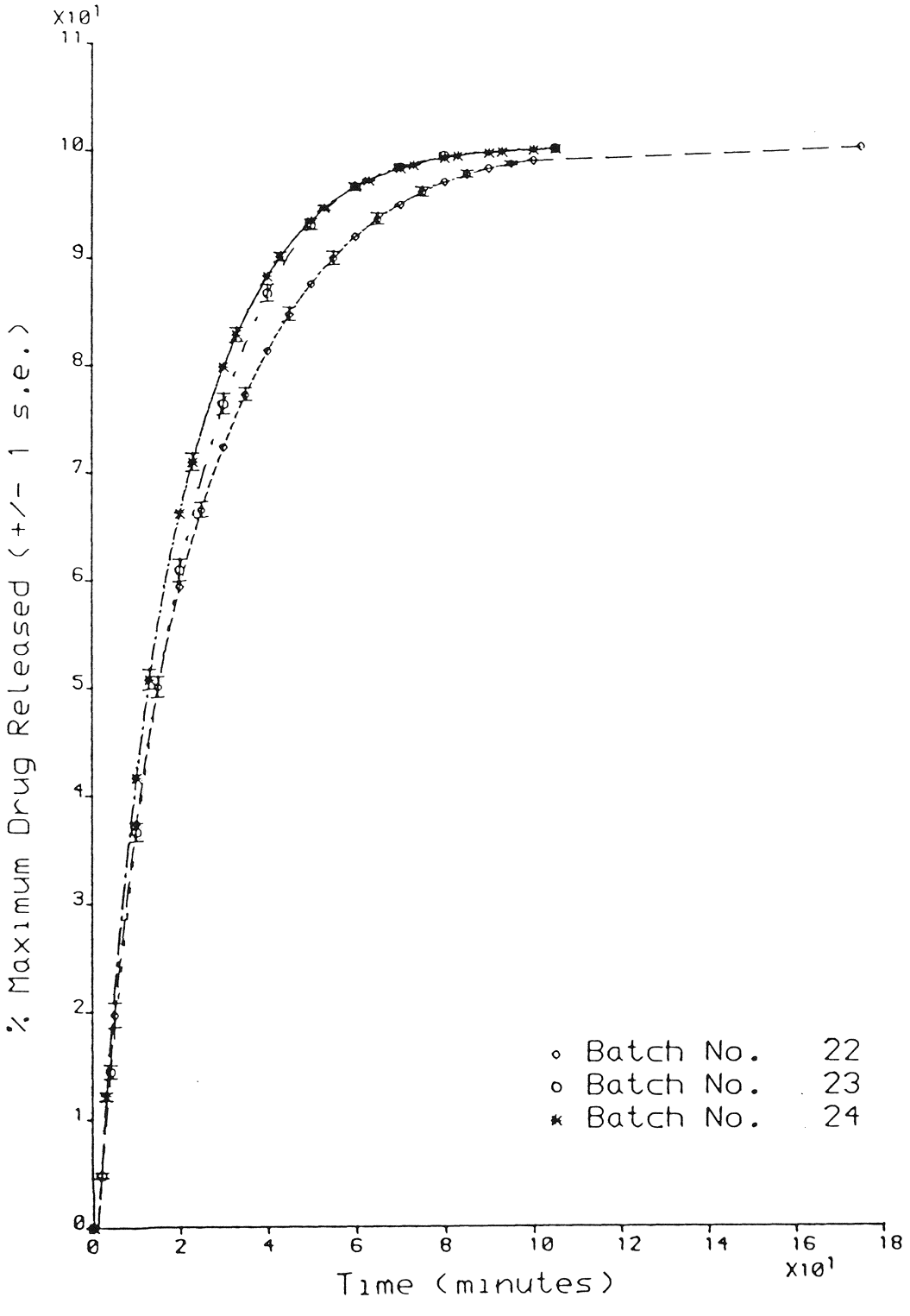

FIGURE 3.17

THE MEAN DISSOLUTION PROFILES FROM THREE BATCHES OF ASPIRIN TABLETS (N=6).

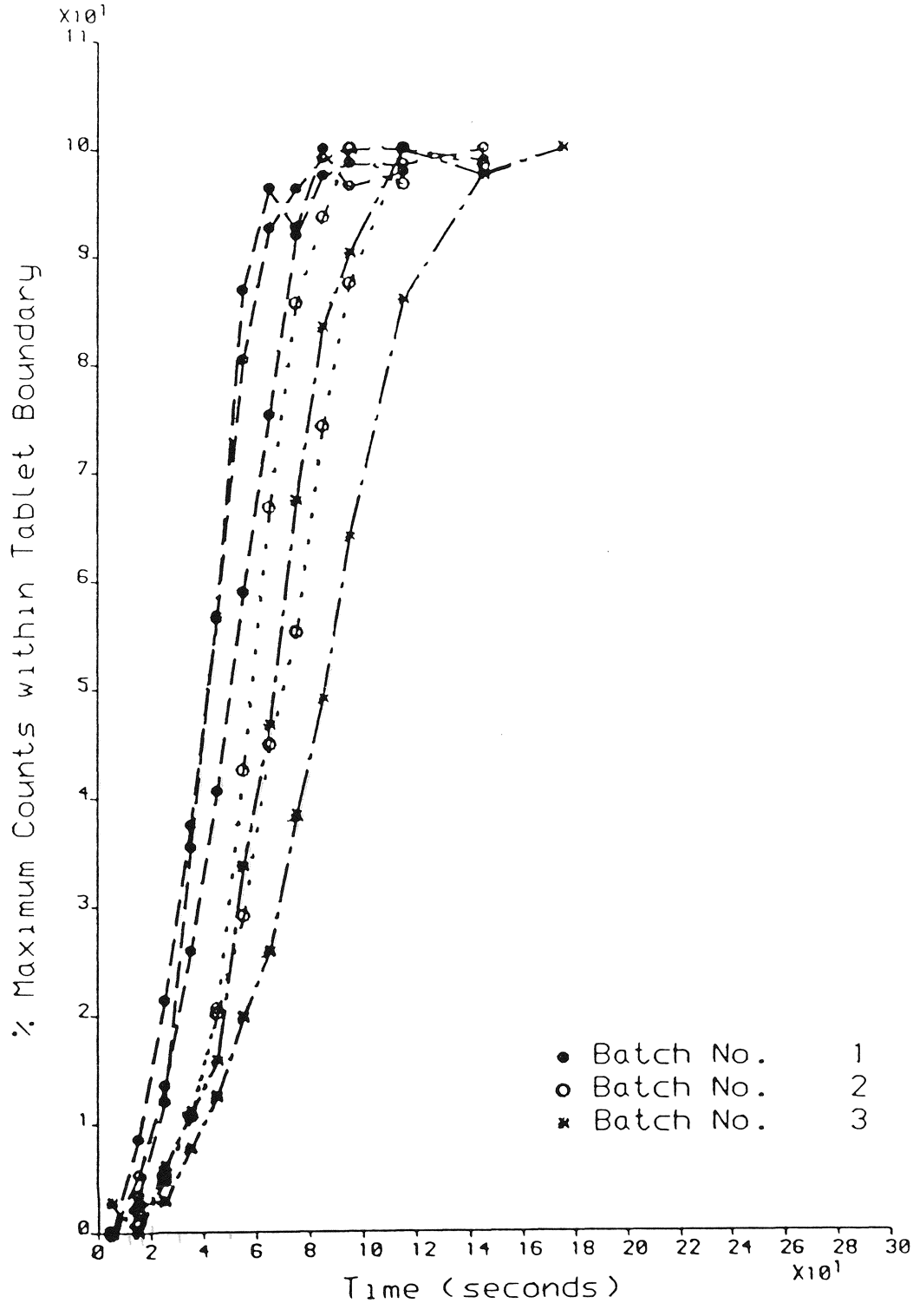

FIGURE 3.18

THE LIQUID UPTAKE INTO PARACETAMOL TABLETS DETERMINED BY GAMMA SCINTIGRAPHY

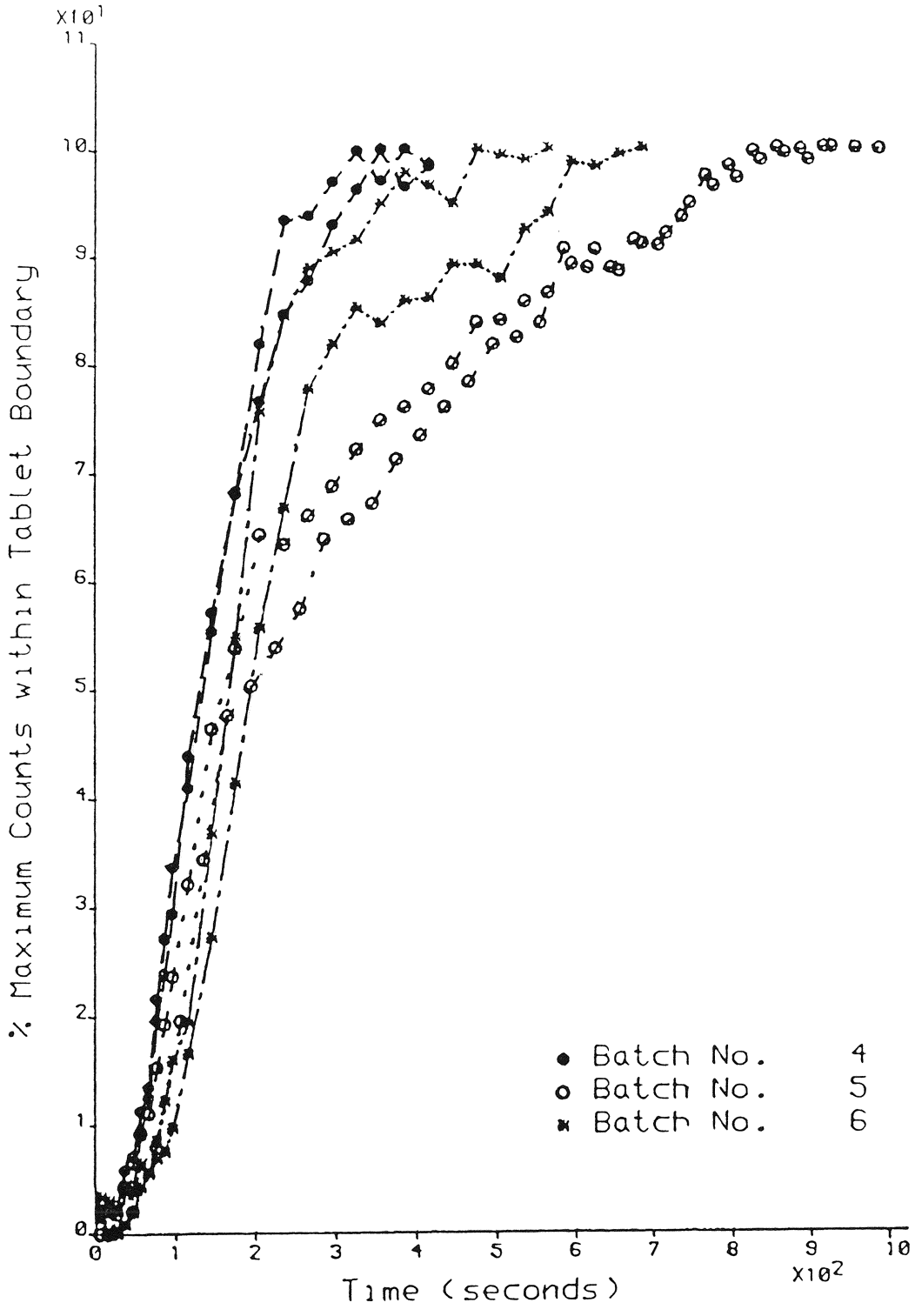

FIGURE 3.19

THE LIQUID UPTAKE INTO PARACETAMOL TABLETS DETERMINED BY GAMMA SCINTIGRAPHY

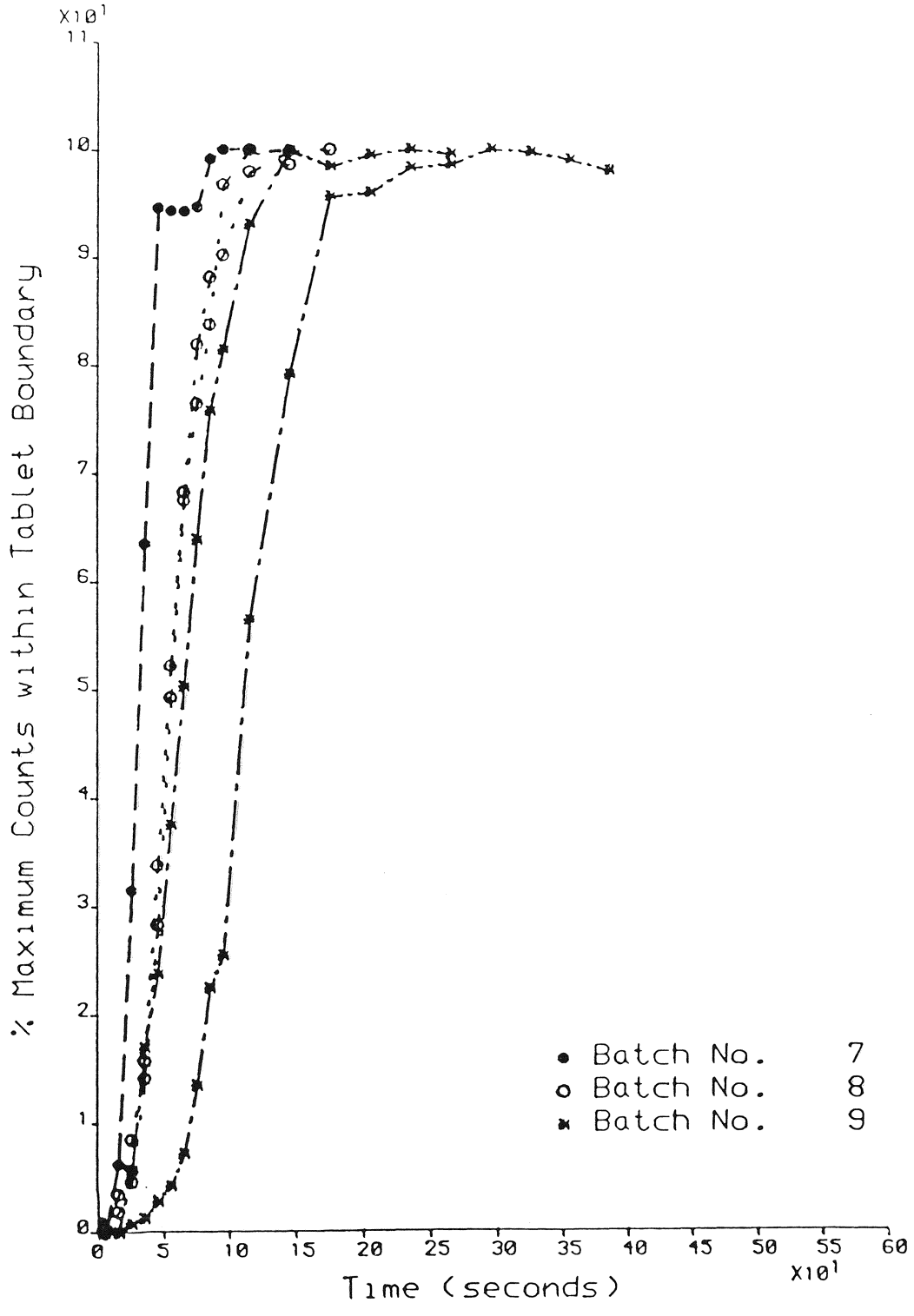

FIGURE 3.20

THE LIQUID UPTAKE INTO PARACETAMOL TABLETS DETERMINED BY GAMMA SCINTIGRAPHY

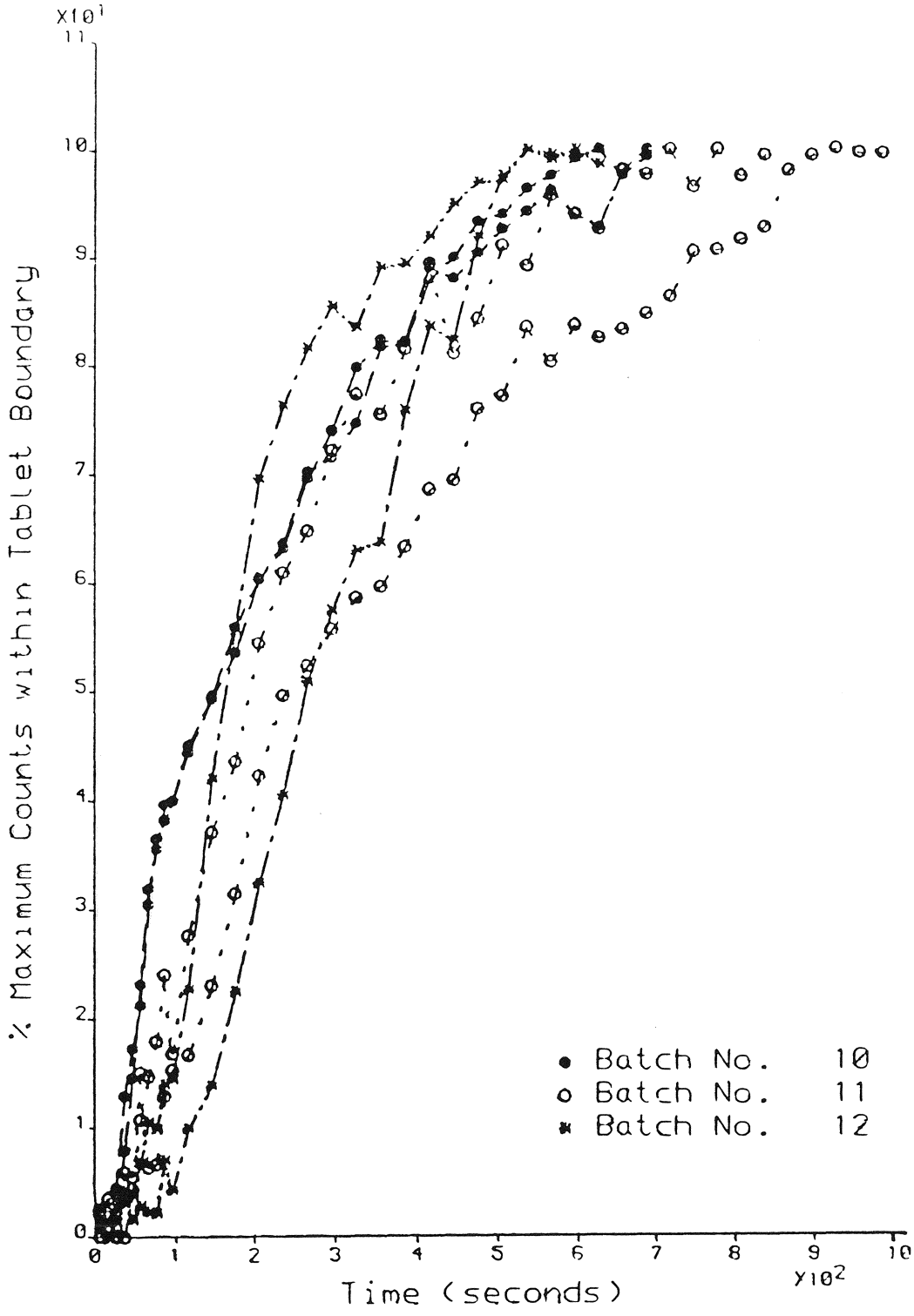

FIGURE 3.21

THE LIQUID UPTAKE INTO PARACETAMOL TABLETS DETERMINED BY GAMMA SCINTIGRAPHY

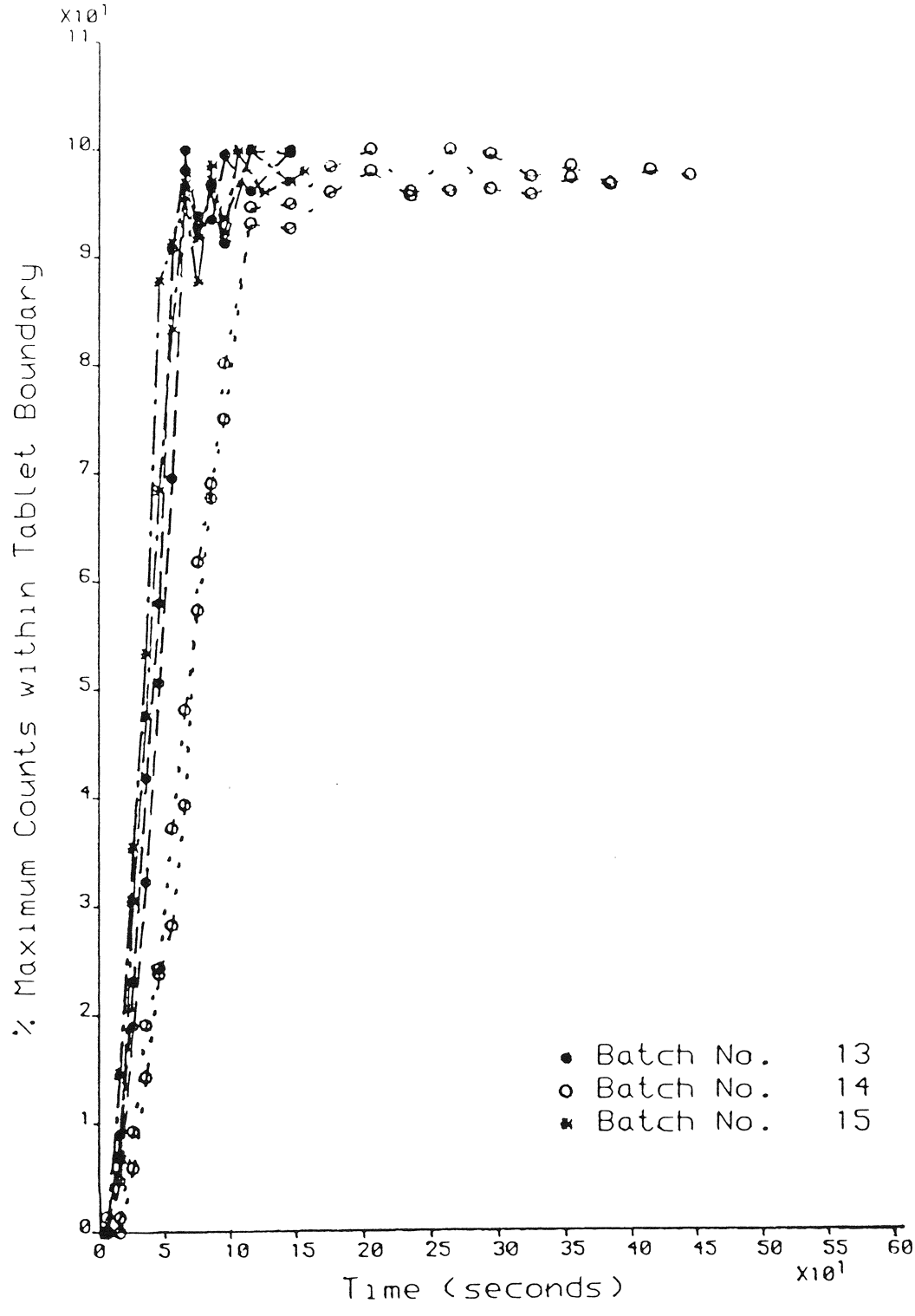

FIGURE 3.22

THE LIQUID UPTAKE INTO PARACETAMOL TABLETS DETERMINED BY GAMMA SCINTIGRAPHY

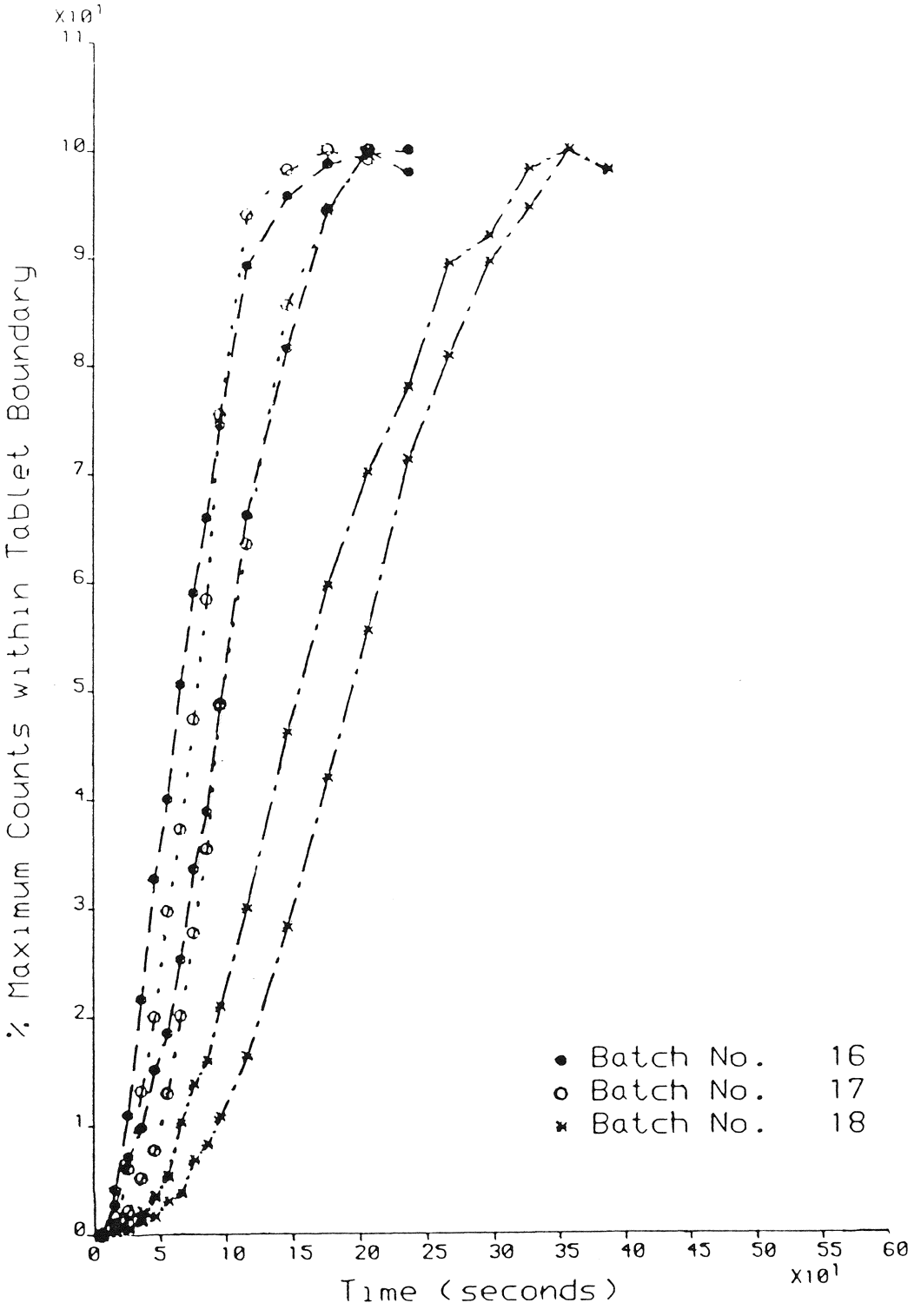

FIGURE 3.23

THE LIQUID UPTAKE INTO PARACETAMOL TABLETS DETERMINED BY GAMMA SCINTIGRAPHY

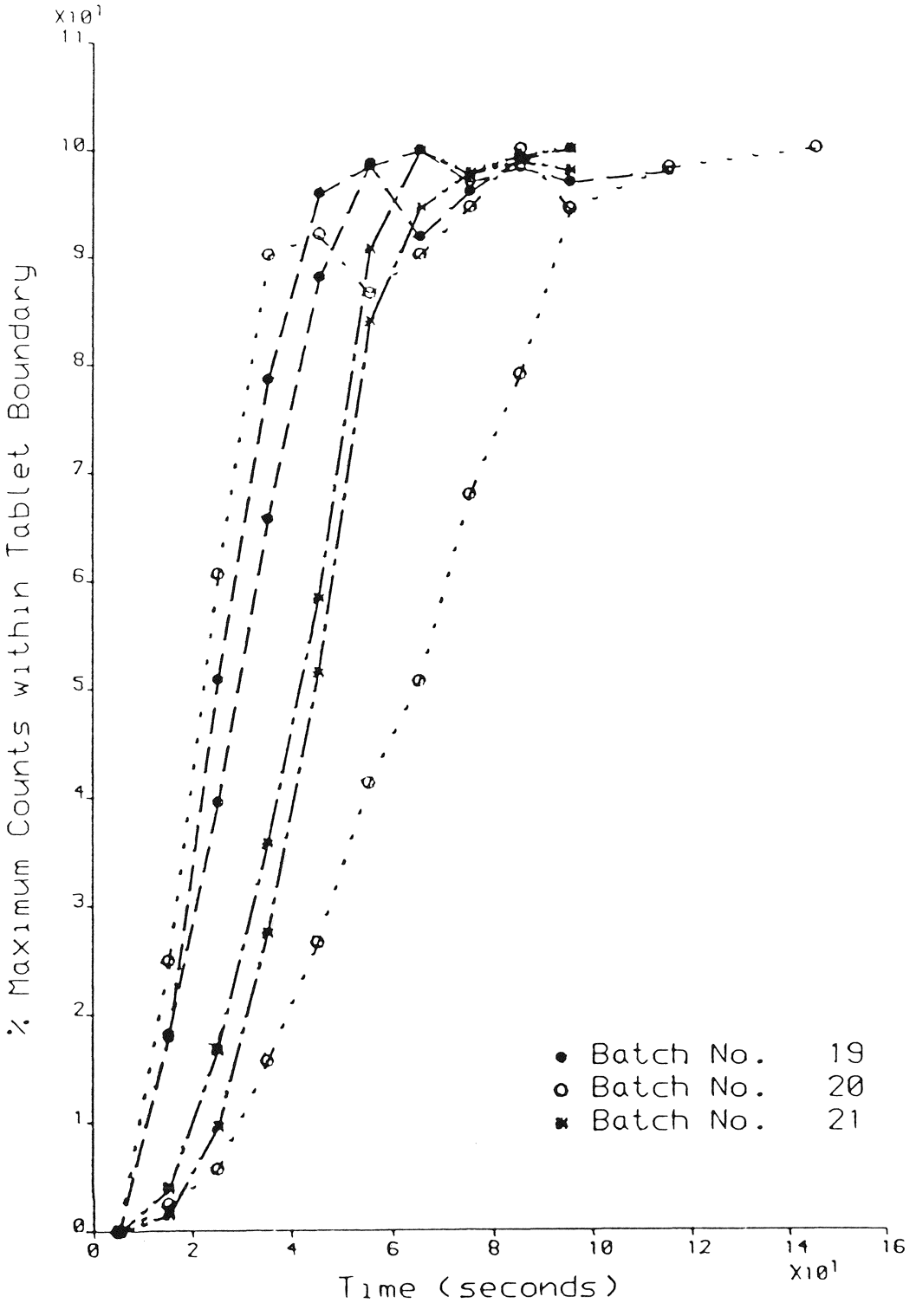

FIGURE 3.24

THE LIQUID UPTAKE INTO PARACETAMOL TABLETS DETERMINED BY GAMMA SCINTIGRAPHY

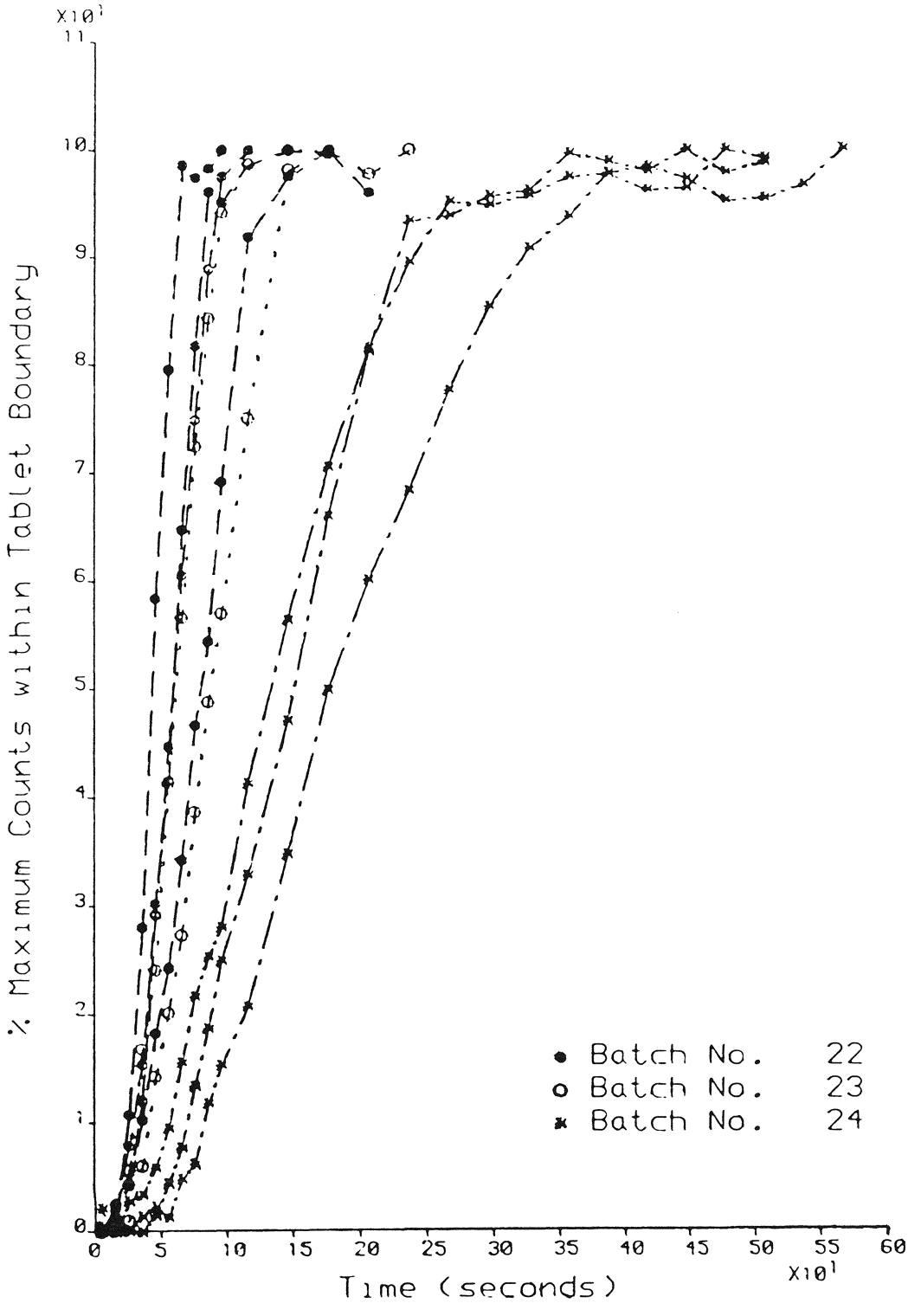

FIGURE 3.25

THE LIQUID UPTAKE INTO PARACETAMOL TABLETS DETERMINED BY GAMMA SCINTIGRAPHY

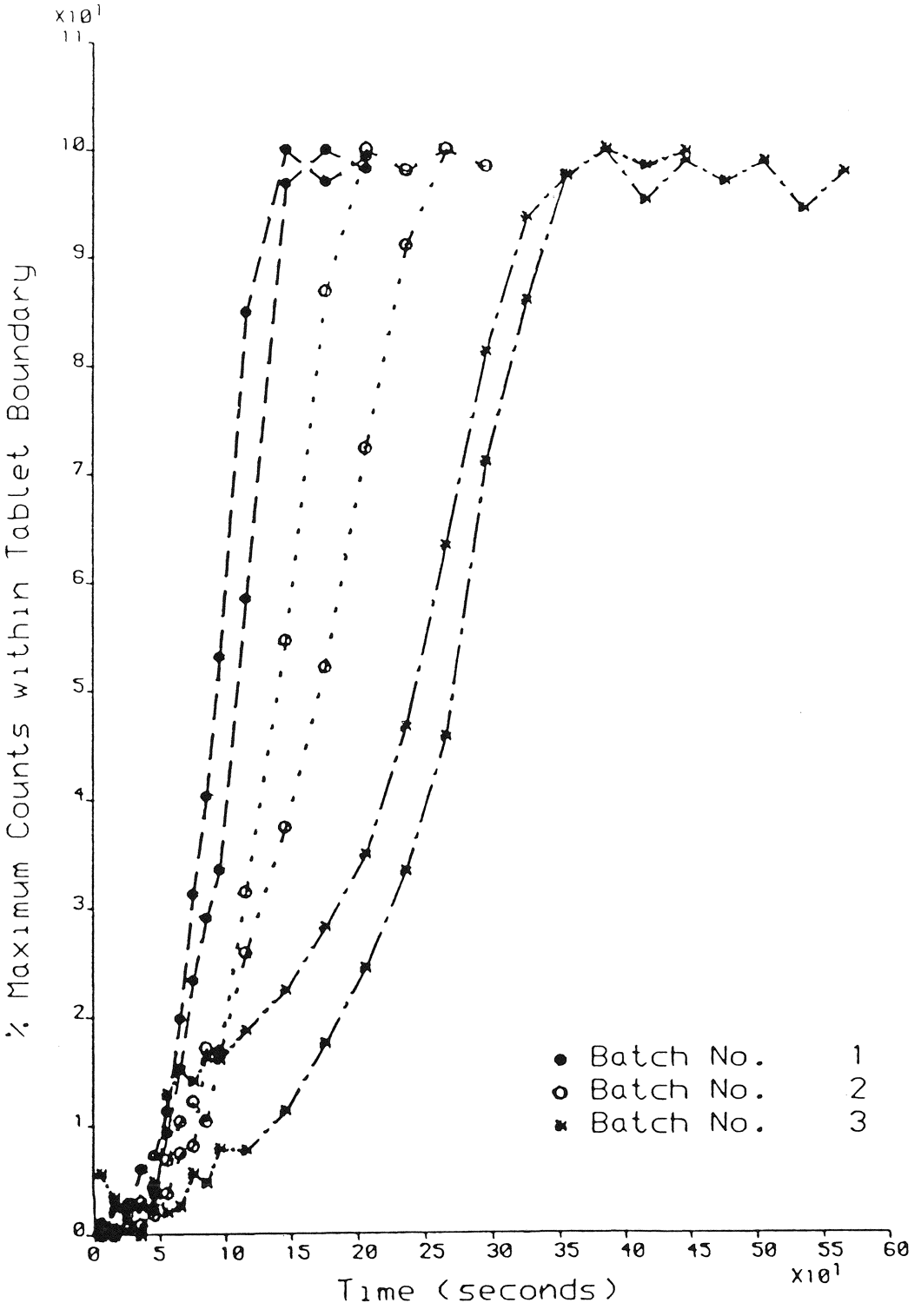

FIGURE 3.26

THE LIQUID UPTAKE INTO ASPIRIN TABLETS DETERMINED BY GAMMA SCINTIGRAPHY

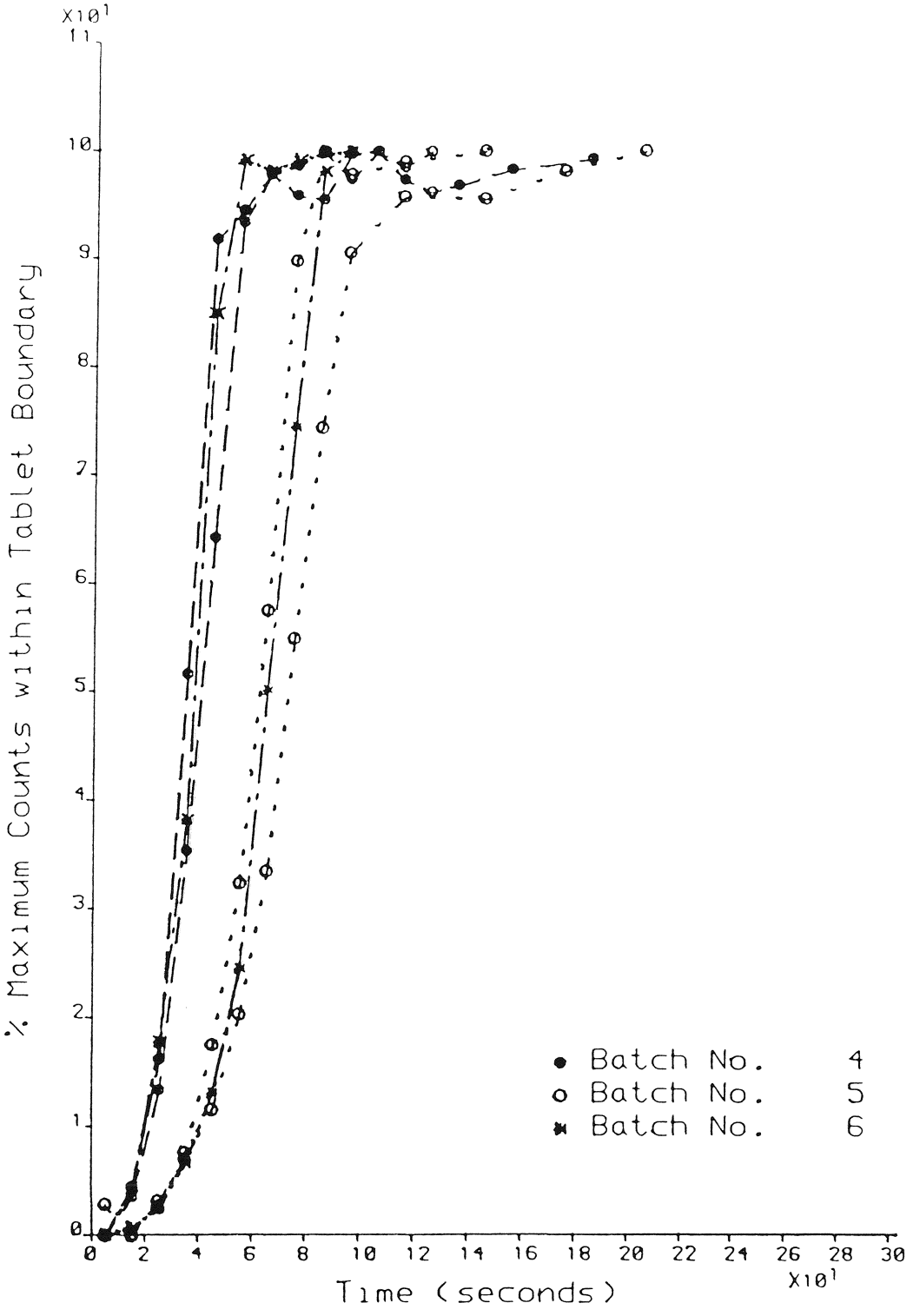

FIGURE 3.27

THE LIQUID UPTAKE INTO ASPIRIN TABLETS DETERMINED BY GAMMA SCINTIGRAPHY

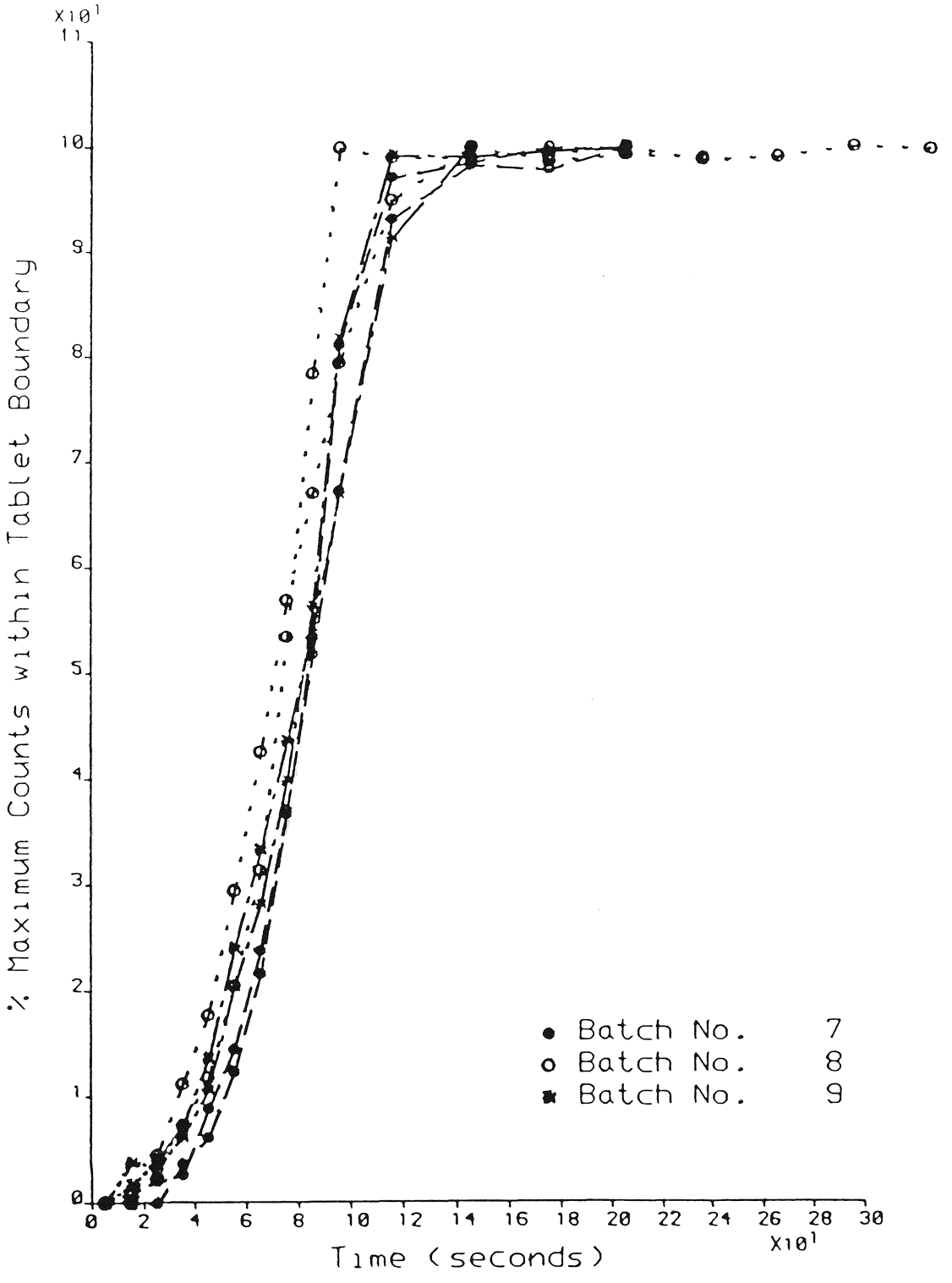

FIGURE 3.28

THE LIQUID UPTAKE INTO ASPIRIN TABLETS DETERMINED BY GAMMA SCINTIGRAPHY

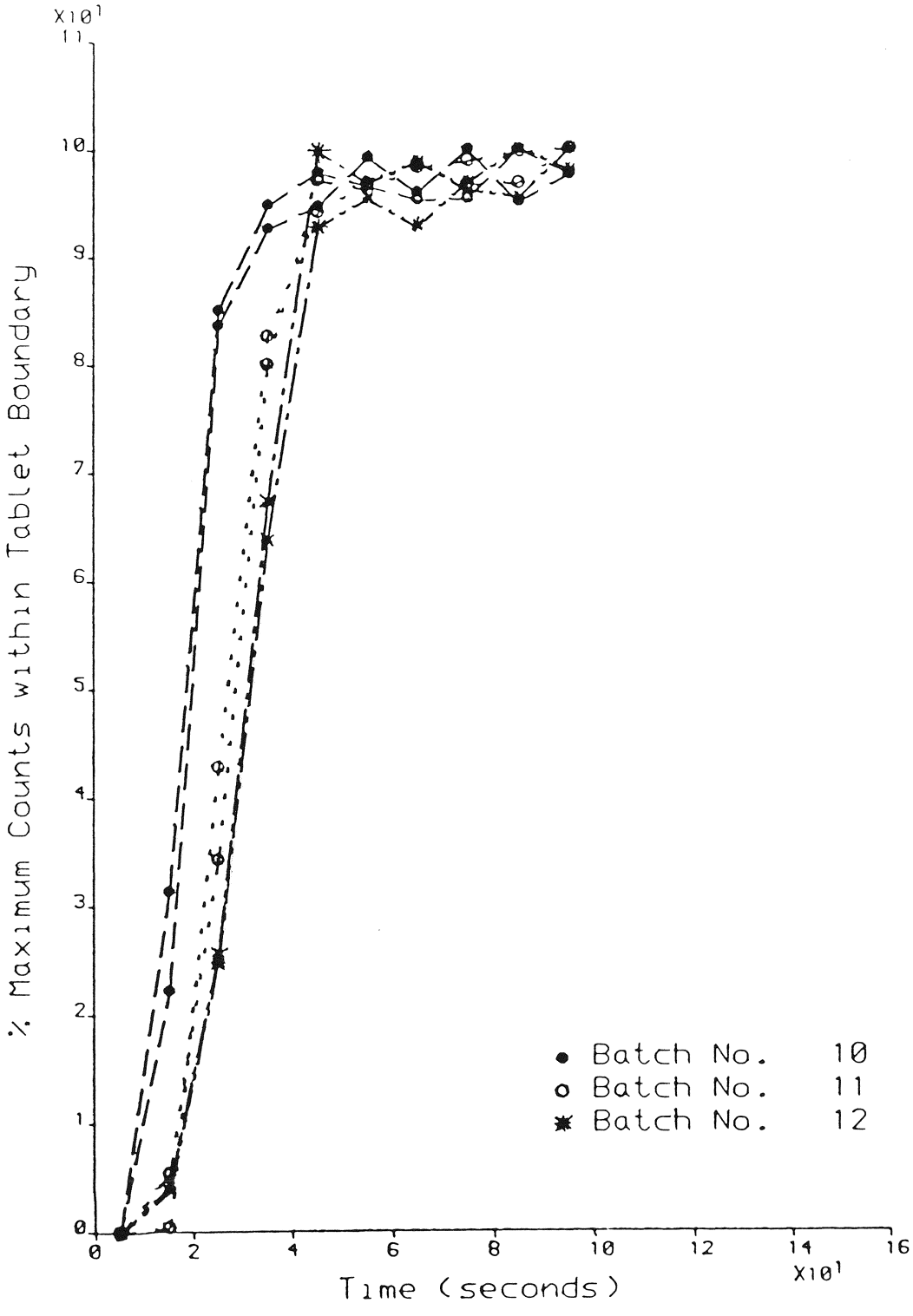

FIGURE 3.29

THE LIQUID UPTAKE INTO ASPIRIN TABLETS DETERMINED BY GAMMA SCINTIGRAPHY

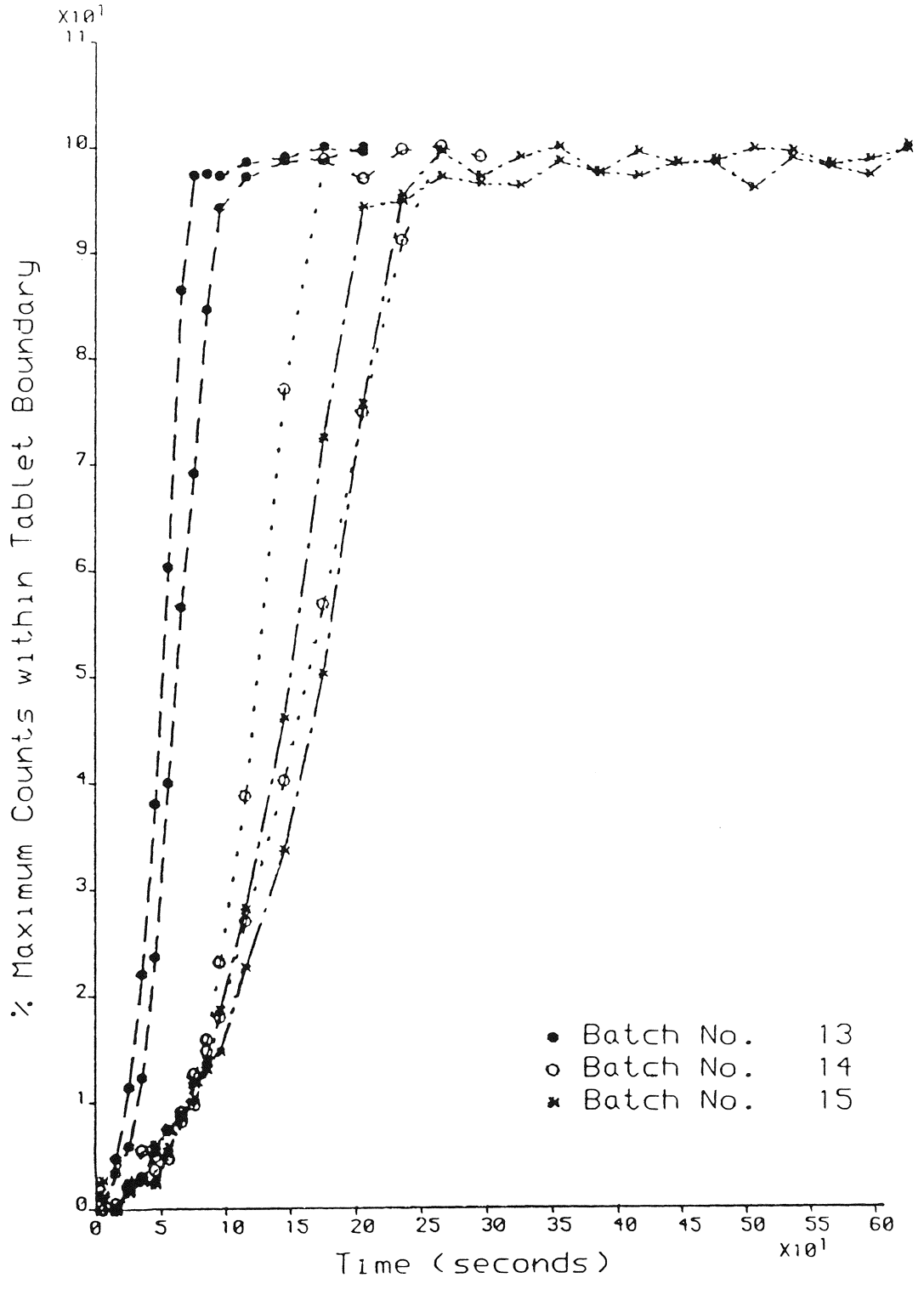

FIGURE 3.30

THE LIQUID UPTAKE INTO ASPIRIN TABLETS DETERMINED BY GAMMA SCINTIGRAPHY

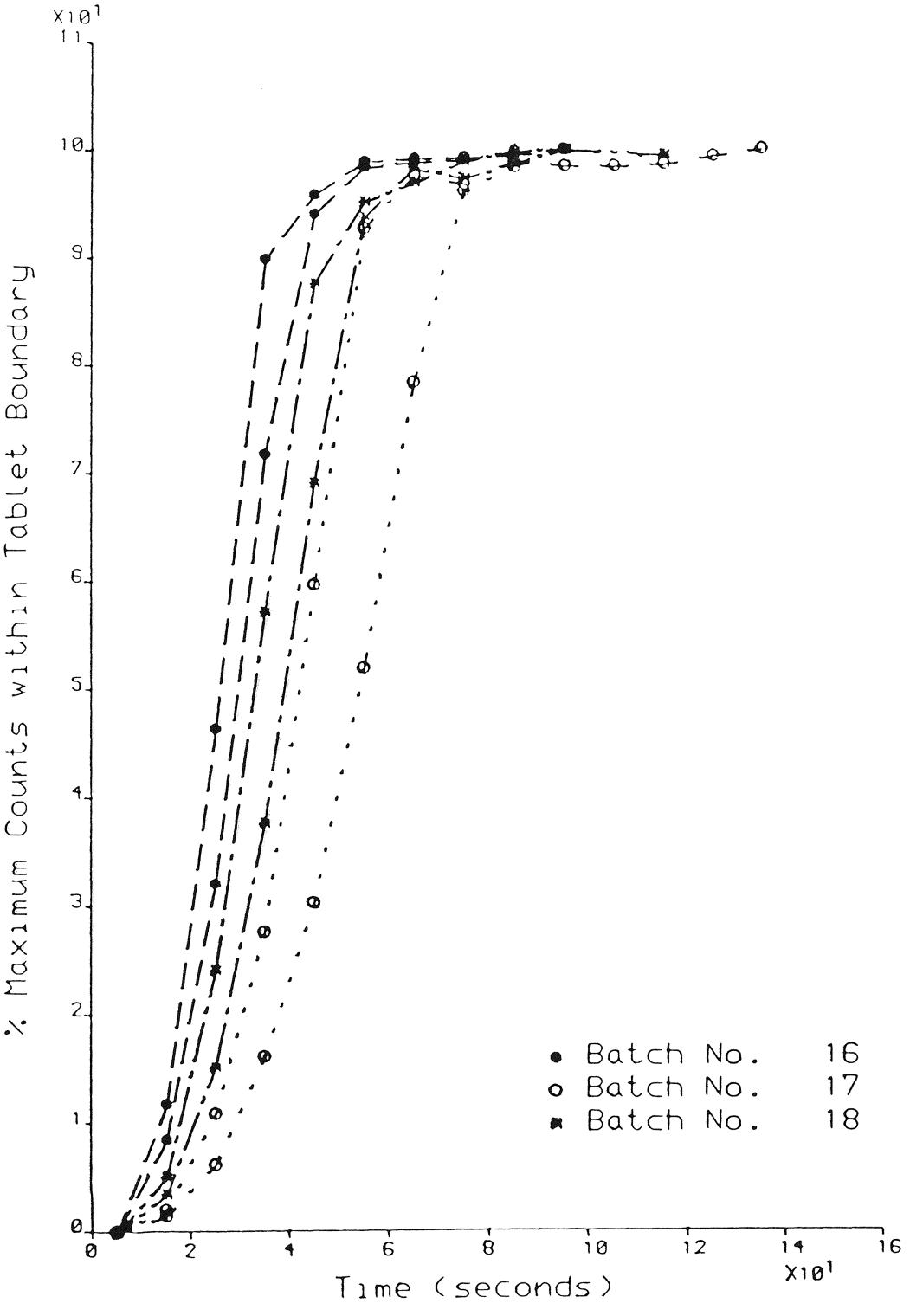

FIGURE 3.31

THE LIQUID UPTAKE INTO ASPIRIN TABLETS DETERMINED BY GAMMA SCINTIGRAPHY

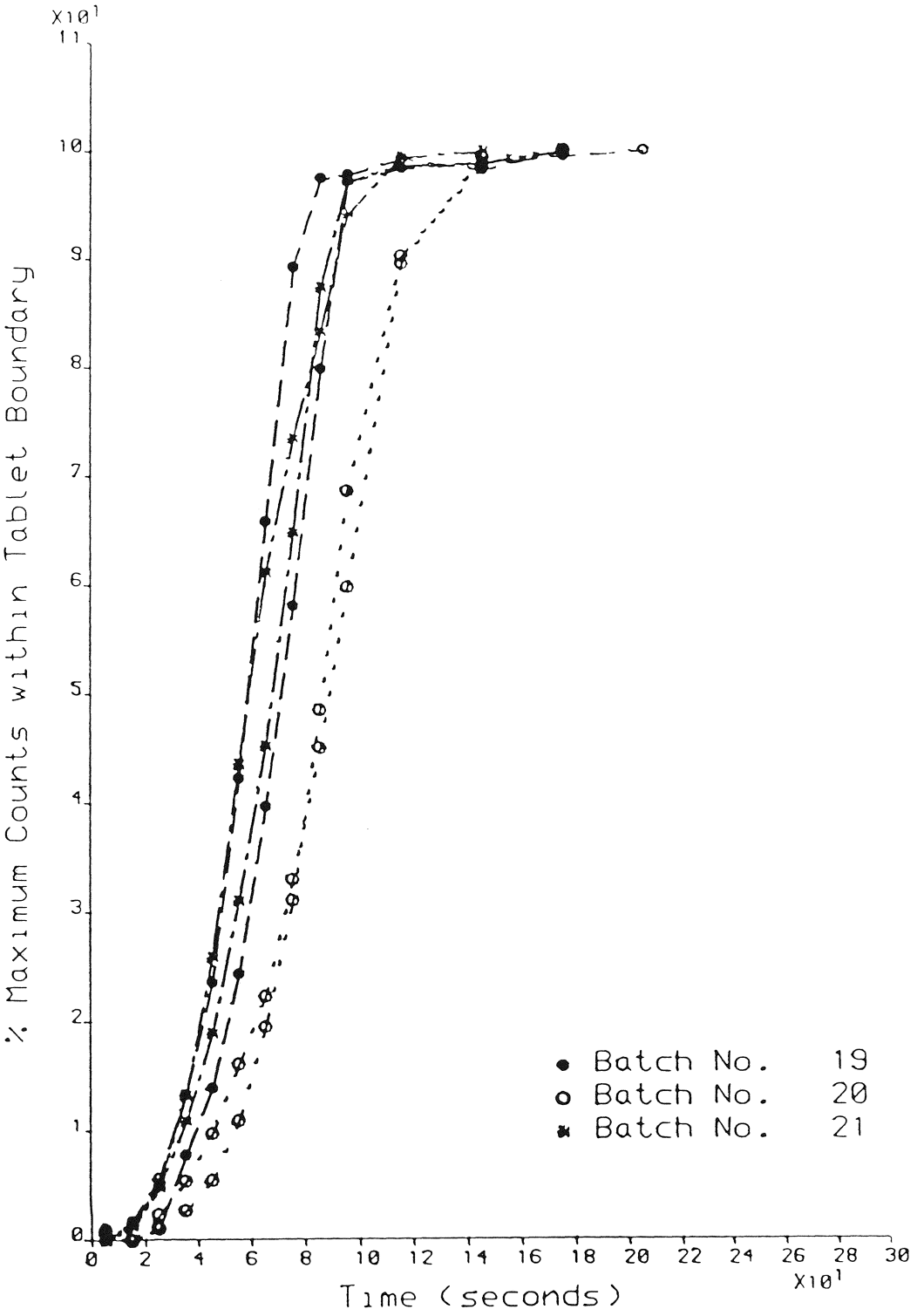

FIGURE 3.32

THE LIQUID UPTAKE INTO ASPIRIN TABLETS DETERMINED BY GAMMA SCINTIGRAPHY

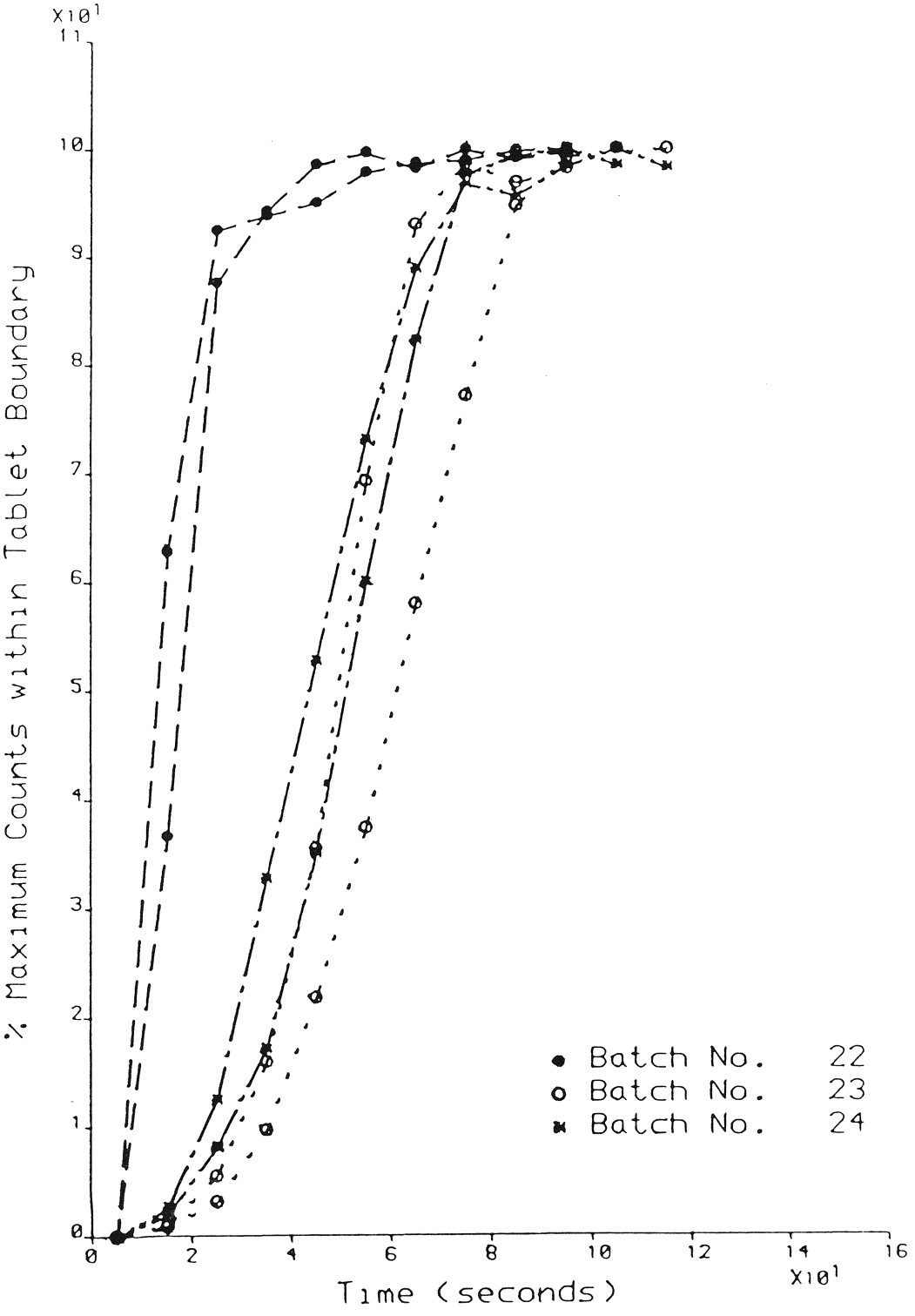

FIGURE 3.33

THE LIQUID UPTAKE INTO ASPIRIN TABLETS DETERMINED BY GAMMA SCINTIGRAPHY

IDENTIFIER	MINIMUM	MEAN	MAXIMUM	VALUES	MISSING
UPP	88.6	147.5	214.9	24	0

1

***** ANALYSIS OF VARIANCE *****

VARIATE: UPP

SOURCE OF VARIATION	DF	SS	SS%	MS	VR
UNITS STRATUM					
MIXTIME	1	94.01	0.24	94.01	1.713
STARCH	1	4.77	0.01	4.77	0.087
SIZE	1	422.52	1.07	422.52	7.699
PRESS	2	37283.72	94.45	18641.86	339.691
MIXTIME.STARCH	1	25.01	0.06	25.01	0.456
MIXTIME.SIZE	1	177.67	0.45	177.67	3.238
STARCH.SIZE	1	20.35	0.05	20.35	0.371
MIXTIME.PRESS	2	274.09	0.69	137.05	2.497
STARCH.PRESS	2	620.47	1.57	310.23	5.653
SIZE.PRESS	2	91.88	0.23	45.94	0.837
MIXTIME.STARCH.SIZE	1	5.13	0.01	5.13	0.094
MIXTIME.STARCH.PRESS	2	32.94	0.08	16.47	0.300
MIXTIME.SIZE.PRESS	2	165.24	0.42	82.62	1.506
STARCH.SIZE.PRESS	2	145.73	0.37	72.86	1.328
RESIDUAL	2	109.76	0.28	54.88	
TOTAL	23	39473.28	100.00	1716.23	
GRAND TOTAL	23	39473.28	100.00		

GRAND MEAN 147.5
TOTAL NUMBER OF OBSERVATIONS 24

***** TABLES OF MEANS *****

VARIATE: UPP

GRAND MEAN 147.5

MIXTIME	1	5
	149.5	145.6

STARCH	5	35
	148.0	147.1

SIZE	large	small
	151.7	143.4

PRESS	100	150	200
	99.9	146.4	196.4

IDENTIFIER	MINIMUM	MEAN	MAXIMUM	VALUES	MISSING
UPP	93.7	153.7	226.1	24	0

1

***** ANALYSIS OF VARIANCE *****

VARIATE: UPP

SOURCE OF VARIATION	DF	SS	SS%	MS	VR
UNITS STRATUM					
MIXTIME	1	64.68	0.16	64.68	3.051
STARCH	1	4.17	0.01	4.17	0.197
SIZE	1	148.01	0.36	148.01	6.982
PRESS	2	37969.62	92.36	18984.81	895.565
MIXTIME.STARCH	1	130.67	0.32	130.67	6.164
MIXTIME.SIZE	1	266.67	0.65	266.67	12.579
STARCH.SIZE	1	0.88	0.00	0.88	0.042
MIXTIME.PRESS	2	39.74	0.10	19.87	0.937
STARCH.PRESS	2	73.94	0.18	36.97	1.744
SIZE.PRESS	2	145.94	0.35	72.97	3.442
MIXTIME.STARCH.SIZE	1	191.53	0.47	191.53	9.035
MIXTIME.STARCH.PRESS	2	725.22	1.76	362.61	17.105
MIXTIME.SIZE.PRESS	2	1280.86	3.12	640.43	30.211
STARCH.SIZE.PRESS	2	28.15	0.07	14.07	0.664
RESIDUAL	2	42.40	0.10	21.20	
TOTAL	23	41112.45	100.00	1787.50	
GRAND TOTAL	23	41112.45	100.00		

GRAND MEAN 153.73
TOTAL NUMBER OF OBSERVATIONS 24

***** TABLES OF MEANS *****

VARIATE: UPP

GRAND MEAN 153.73

MIXTIME	1	5
	155.37	152.08

STARCH	5	35
	153.31	154.14

SIZE	large	small
	156.21	151.24

PRESS	100	150	200
	102.69	158.76	199.73